ANALYSIS OF PAVEMENT CONDITION DATA EMPLOYING PRINCIPAL COMPONENT ANALYSIS AND SENSOR FUSION TECHNIQUES

by

KRITHIKA RAJAN

B.E., Anna University, India, 2006

A THESIS

submitted in partial fulfillment of the

requirements for the degree

MASTER OF SCIENCE

Department of Electrical and Computer Engineering

College of Engineering

KANSAS STATE UNIVERSITY

Manhattan, Kansas

2008

Approved by:

Co-Major Professor
Balasubramaniam Natarajan

Approved by:

Co-Major Professor
Dwight D.Day

ABSTRACT

This thesis presents an *automated* pavement crack detection and classification system via image processing and pattern recognition algorithms. Pavement crack detection is important to the Departments of Transportation around the country as it is directly related to maintenance of pavement quality. Manual inspection and analysis of pavement distress is the prevalent method for monitoring pavement quality. However, inspecting miles of highway sections and analyzing each is a cumbersome and time consuming process. Hence, there has been research into automating the system of crack detection. In this thesis, an automated crack detection and classification algorithm is presented. The algorithm is built around the statistical tool of Principal Component Analysis (PCA). The application of PCA on images yields the primary features of cracks based on which, cracked images are distinguished from non-cracked ones.

The algorithm consists of three levels of classification: a) pixel-level b) subimage (32×32 pixels) level and c) image level. Initially, at the lowermost level, pixels are classified as cracked/non-cracked using adaptive thresholding. Then the classified pixels are grouped into subimages, for reducing processing complexity. Following the grouping process, the classification of subimages is validated based on the decision of a Bayes classifier. Finally, image level classification is performed based on a subimage profile generated for the image. Following this stage, the cracks are further classified as sealed/unsealed depending on the number of sealed and unsealed subimages. This classification is based on the Fourier transform of each subimage. The proposed algorithm detects cracks aligned in longitudinal as well as transverse directions with respect to the wheel path with high accuracy. The algorithm can also be extended to detect block cracks, which comprise of a pattern of cracks in both alignments.

ACKNOWLEDGEMENTS

The research work presented here is sponsored by the KDOT under its Kansas Transportation and New Developments (K-TRAN) program. We gratefully acknowledge KDOT's support and guidance.

TABLE OF CONTENTS

LIST OF FIGURES

LIST OF TABLES

Chapter 1

Introduction

This chapter introduces the background, motivation and key contributions of the research presented in this thesis.

1.1 Background

Pavement distress analysis is one of the labor intensive tasks of Departments of Transportation (DOT) around the country. This is because, maintenance of ride quality for highway users includes determining pavement repair requirements in a timely fashion on a regular basis. Hence, DOTs across the country employ various strategies to diligently inspect sections of highways, collect information on pavement conditions and process it to extract meaningful data. Traditionally, manual inspection and data gathering has been the method of choice for detecting pavement damage. In such a system, trained experts walk or drive on highways that are to be inspected. Upon encountering a distress, the data is manually entered on a computer log. This process is not only cumbersome and time consuming but also involves a certain amount of risk, since the traffic flow on highways is hindered. In order to implement better data collection and processing, researchers migrated to automated analysis systems. Here, data collection is performed using specially equipped vehicles driving at highway

speed and recording information such as road profiles and pavement images. These are stored on high capacity computers to be retrieved and processed later. Yet again, manual intervention is required to assimilate road condition information by observing the vast amount of data stored on the computers. Though risk free, this is still a tedious process. Hence, research is currently focussed on automating the process of analyzing stored data. Image processing has emerged as a popular tool in this process. With vehicles equipped with advanced camera and lighting systems, processing pavement images at highway speeds is now possible. The next phase of development involves analyzing these images and detecting pavement distress automatically.

Pavement distresses are a broad category of different anomalous phenomena occurring on pavements. These affect ride quality to different extents. Generally, distresses include cracking, patching and potholes, surface deformation (rutting and shoving), surface defects (bleeding, raveling and so on) and miscellaneous distresses. The Federal Highway Administration has published a Distress Identification Manual that lists the different types of distresses and the characteristics of each [1]. The primary focus of this thesis is on detecting cracking phenomenon and classifying its severity. The major types of cracks are transverse, longitudinal, block and fatigue. Further explanation on each of these is provided in chapter 2. In the next section, the prior research performed and the motivation behind the thesis are presented.

1.2 Motivation for this thesis

The necessity for automating the process of analyzing pavement condition data generated by imaging vehicles cannot be overstated. Analysis of the large amount of data generated by the data collection system manually is impractical and time-consuming. In [2], cracks are manually detected on pavements and the suspect regions are photographed. The images captured are then processed manually using a software to

segment cracked sections. It is evident that this process would be intractable for implementation on long sections of highways. Moreover, it would also be inconsistent due to operator errors. Hence, to eliminate such a tedious process and improve detection accuracy, researchers have focussed their efforts on effective image processing techniques to automatically detect cracks, with minimal or no human interaction.

Recently, Yamaguchi and Hashimoto proposed the use of improved percolation modeling as a technique to detect pavement cracks [3]. However, the process in [3] is not completely automated and may require human interaction to set certain seed parameters. From an image processing standpoint, there has been emphasis on preprocessing to remove noise while retaining already tested methods of crack detection [4]. The effectiveness of the proposed preprocessing technique was analyzed by testing 50 noisy concrete images. The authors in [4] mainly emphasize preprocessing without considering the variation in pavement roughness.Furthermore, the types of cracks present in the test images have not been provided. Hence, it is uncertain whether this system will perform optimally for all types and extents of cracks. In another paper, the Fast Haar wavelet transform is used to detect crack edges on concrete surfaces [5]. To improve the accuracy of the transform, ROC analysis is used to define the optimal parameter set, which includes the threshold for the edge detection algorithm. In [6], the authors propose the use of histogram projection to identify cracks within a cropped image. Histogram projection is the technique of averaging the pixel intensities in each row/column and smoothing the difference from a reference gray level. While [6] focussed on the severity of cracks, crack classification (in terms of sealed or unsealed), was not performed. Moreover, the system in [6] cannot detect multiple cracks within an image. In a research undertaken by the Texas Department of Transportation, pavement images were divided into grid cells of 8×8 pixels each, called seeds, and detection and classification were performed on the seeds [7]. A connection algorithm was used to cluster seeds in a linear string and thus detect transverse and

longitudinal cracks. Though this process is computationally not very complex, the performance may become poor for certain degrees of pavement roughness. For instance, on a rough surface, the contrast between the pixel intensities of a mild crack and neighboring background pixels may not be significant. In this case, the algorithm in [7] might not detect the crack. Thus, pixel intensity alone is not a robust feature for detecting cracks. In a paper by Bray [8], detection of cracks is performed using a neural network while classification is performed by another neural network. The proposed algorithm has not been tested on real images. The artificially generated images may not yield a good picture of the computational complexity of the algorithm nor of the effectiveness of the technique on real images. Though there are some commercial software such as WiseCrax developed by Roadware Group Inc.[9] that can perform automated crack detection, their performance cannot be guaranteed. The results produced from these software do not meet the requirements of KDOT. For example, existing software solutions do not integrate profile data and image analysis, a feature that is desirable for quantifying the severity of cracks.

In [10], researchers at Utah State University (USU), in collaboration with the Utah Department of Transportation (UDOT), present a real time automated crack detection and classification system. Here, fuzzy logic has been used to detect distresses followed by a neural network that classifies the distress. It is well known that neural classifiers tend to perform poorly when test data deviates from training data. Therefore, the authors' claim of high classifying accuracy is not well substantiated with a test set of just 42 images in [11]. Additionally, the sensitivity of the approach to variable operating conditions (for example, non-uniform lighting and varying pavement surface roughness) has not been analyzed. Neural networks have also been applied in [12] to classify pavement distresses. While the training data is artificially generated, the testing data comprises of both artificial and actual pavement images. However, the number of actual pavement images (83) is not large

enough for the conclusive evaluation of the technique. In [13] also neural networks are used to perform pavement distress detection and classification.

In a paper by Iyer and Sinha [14], image processing is used to segment cracking in underground pipes. Though this field of study is different from pavement analysis, the principles behind crack detection are identical. A contrast enhancement algorithm has been applied in this paper, followed by the application of morphology. The algorithms are adapted to account for pipe characteristics and appear to perform well. Hence, they may not be directly applicable to pavement images.

Therefore, a completely automated crack detection/classification system that can classify all types of cracks is still an open problem. For practical adoption of any new technology, the detection system should be efficient, affordable and accurate. The research described in this thesis pertains to developing such a system for the Kansas Department of Transportation. Real pavement images were provided by KDOT. The algorithm developed using image processing and pattern recognition concepts is presented in the following chapters. The next section presents the key contributions of the thesis, while briefly introducing the steps in the algorithm.

1.3 Key Contributions

This section briefly describes the novel algorithm developed and the key contributions of the thesis.

The focus of this thesis is on developing a fully automated system that can read images stored in the database and process each image. The objective of this system is to detect and classify cracks in an image, presenting cracks localized within an image and discarding non-cracked images. Moreover, all types of cracks under different pavement roughness conditions are to be classified with high accuracy. Our proposed algorithm will reduce the labor involved in analyzing each image manually

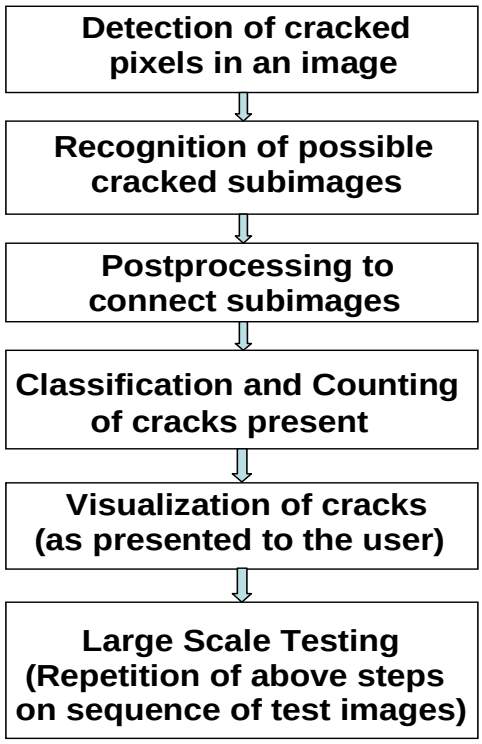

Figure 1.1: A Flowchart of the algorithm

and identifying images with cracks without the aid of any pattern recognition software. The proposed algorithm consists of four stages namely (1) detection; (2) recognition; (3) postprocessing, and (4) visualization. A flowchart indicating the sequence is shown in figure 1.1. The stages in this algorithm are explained in the following chapters.

Each test image is processed through the above stages sequentially and the final output image is presented to the end analyst along with the system's observation on the cracked nature of the image.

The key contributions of the thesis are summarized below:

- The proposed algorithm is capable of detecting mild as well as severe transverse and longitudinal cracks.
- The detection stage, described in chapter 3, efficiently filters out most of the unconnected background noise and presents a more relevant image to the suc-

cessive stages.

- In the classification stage, pixels are grouped into subimages to reduce the complexity of further processing. The grouping process is presented in Section 4.1. The classification of subimages is validated using a Bayes classifier presented in Section 4.2. This stage performs further filtering of subimages that do not contain a significant percent of cracked pixels.

- In the recognition stage, the technique of Principal Component Analysis(PCA) has been applied to extract the weights associated with the cracked/non-cracked nature of a subimage. The extracted weights and the developed classifier work extremely well to distinguish between cracked and non-cracked subimages.

- Chapter 5 describes the postprocessing used to connect up cracked subimages that are not well connected and remove isolated subimages. Such cases of missing connectivity do occur frequently, especially in cracks that are mild. A final filtering process is applied to the image at this stage.

- Section 6.1, describes the metric used to automatically recognize a crack and localize it within an image. This metric works well to identify the region in which a crack is present. Even multiple cracks within an image are located accurately in this stage.

- Once the region of the crack has been identified, the crack is further classified as sealed or unsealed, in the case of transverse cracks. This classification is important to analysts since the need for repair is determined based on whether the crack has already been attended to by way of sealing. Further information on sealing of cracks is presented in Section 6.2.

- Though the initial focus of the algorithm was on transverse cracks, it also work well on longitudinal cracks. The only modification required is transposing of

images before running them through the whole process so that the algorithm is again presented with cracks running in the transverse direction.

- When tested on a large set of real pavement images, the algorithm is found to have a detection probability of 97.10% for transverse cracks and 94.11% for longitudinal cracks.

- The most important contribution of the thesis is that the developed algorithm is completely automated. The thresholds used are adaptive. Hence, there is no need for human interaction till the whole data set has been processed and the results stored.

To summarize, our algorithm automates the process of crack detection and classification from real pavement images. It can be applied on transverse and longitudinal cracks with a high rate of detection and very low rate of false detection.

1.4 Organization of the thesis

The rest of the thesis is organized as follows : Chapter 2 introduces the classifications of cracking phenomena and the data collection equipment installed in the imaging vehicle; Chapter 3 describes the stage of preprocessing/detection of cracked pixels from an image; Chapter 4 deals with the core recognition process, where subimage level classification is performed; Chapter 5 deals with postprocessing of the image, i.e., the application of morphology to connect cracked subimages and remove isolated subimages; Chapter 6 describes image level classification, sub-classification of cracks present, counting them and presenting the information to the end user for easy visualization, along with large-scale testing results; Chapter 7 presents a discussion on profile data and their significance, with a description of the techniques being considered to analyze them; finally, Chapter 8 presents the conclusion of the thesis, a summary of its key contributions and future research extensions.

1.5 Summary

This chapter presented the background of the research, the prior work done, the motivation for the thesis and its key contributions. In the next chapter, the reader is introduced to different crack classifications and the data collection system.

Chapter 2

Pavement Distress Phenomena

In this chapter, we present the classifications and sub-categories of pavement cracking and the measuring system used to collect pavement images. Image examples for each type of cracking are presented, along with their primary features. Classification of cracks depends on their alignment and structure. Hence, these are the features that have to be intelligently extracted by the algorithm to perform accurate classification. A study of such features aids in the development of an automated classifier. A brief explanation of some of the main characteristics of cracks are presented in this chapter. In Section 2.3, the data collection vehicle is presented. A brief discussion of manual recording of pavement distresses by visual inspection is presented to enforce the necessity of automation. The performance of the measuring system is of utmost importance to pavement maintenance. This is because inaccurate data collection could introduce artifacts into the images captured, which lead to increased complexities of processing algorithms.

2.1 Transverse cracking

Transverse cracks are cracks that run across the width of the pavement surface, i.e., from left to right. Examples of transverse cracks are shown in figure 2.1.

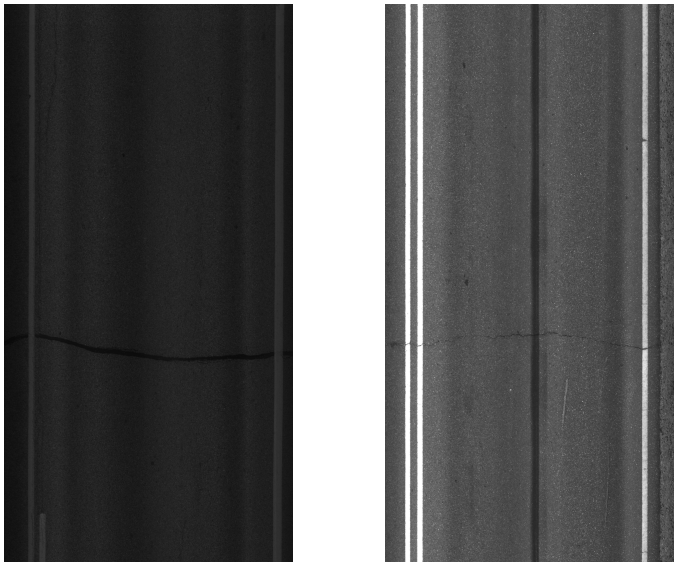

Figure 2.1: (a)Sealed Transverse crack (b)Unsealed Transverse crack

One type of classification of Transverse cracks is based on whether they are sealed or unsealed. Sealed cracks are the ones to which a sealant has been applied in order to control its growth. Further reasons for using sealing as a method of countering cracks can be found in [15]. Hence, this classification indicates to the end user the status of a crack,that is, if it has been already treated or if it requires repair. Some examples of transverse cracks are presented in figure 2.1.

Another way of classifying Transverse cracks is based on severity, which is measured in terms of crack roughness. Roughness of a crack, quantified in terms of the International Roughness Index (IRI), indicates the deviation from a perfectly planar surface [16]. The lower the IRI, the less rough a crack is. In turn, the less it affects ride quality and vehicle dynamics. The classification based on roughness identifies transverse cracks as Code 0,1,2 or 3 cracks.

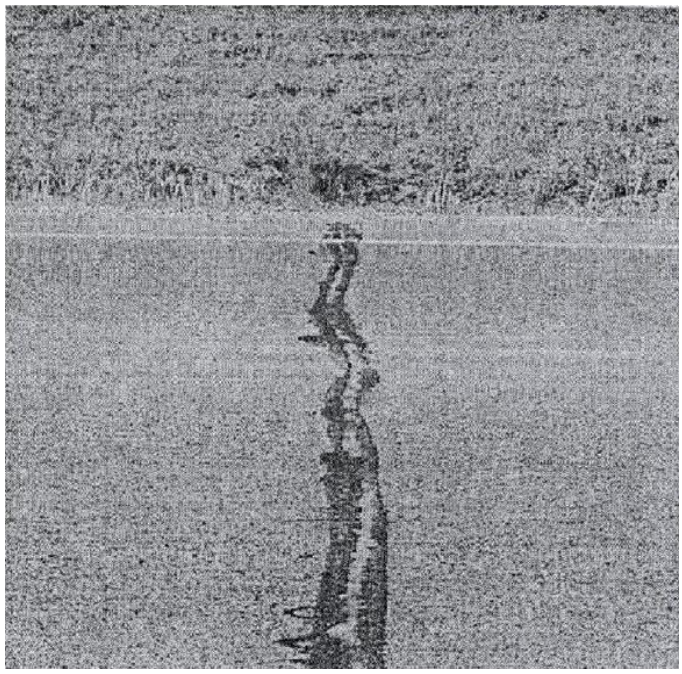

Figure 2.2: A Code 0 transverse crack

- Code 0 cracks are defined as mild cracks that are sealed but have no roughness or break in the sealants. A code 0 crack is represented in figure 2.2.
- Code 1 cracks are sealed/unsealed and with no roughness as shown in figure 2.3.
- Code 2 cracks are sealed/unsealed with noticeable roughness with no depression and of width greater than one inch. Figure 2.4 presents a code 2 transverse crack.
- Code 3 cracks are sealed/unsealed with significant roughness caused by extreme depression. There is also secondary cracking associated with the crack. A Code 3 crack is presented in figure 2.5. Figure 2.6 represents another type of code 3 cracking.

Figure 2.3: A Code 1 transverse crack, $\frac{1}{4}$ inch with no roughness

The descriptions of the coded cracks and the images of each type of cracking shown above have been provided by KDOT [17]. The primary focus of this thesis is on transverse cracks which occur more commonly than other types of cracks. The high frequency of occurrence of transverse cracks also provides large training data that can be utilized to condition the detection algorithm effectively. Moreover, the set of training data comprised of pavement surfaces of different degrees of roughness. Hence, wide variations in the pavement roughness have been accounted for in the algorithm. In the next section, we present a brief description of the other types of cracking which, though not frequent, still occur.

Figure 2.4: A Code 2 transverse crack

2.2 Other cracking phenomena

In this section, we present the characteristics of other types of cracks that occur on pavement surfaces.

2.2.1 Longitudinal cracks

Longitudinal cracks, as the name implies, run along the length of the pavement surface, i.e., in the direction of travel on roads. In other words, longitudinal cracks are perpendicular to transverse cracks. This alignment of longitudinal cracks can be exploited to detect them. Since images are processed by treating them as matrices, a transposed longitudinal crack can be presented as a transverse crack to the detection algorithm. This operation adapts the image for processing by the same algorithm and the rate of detection could be expected to be as accurate as for actual transverse

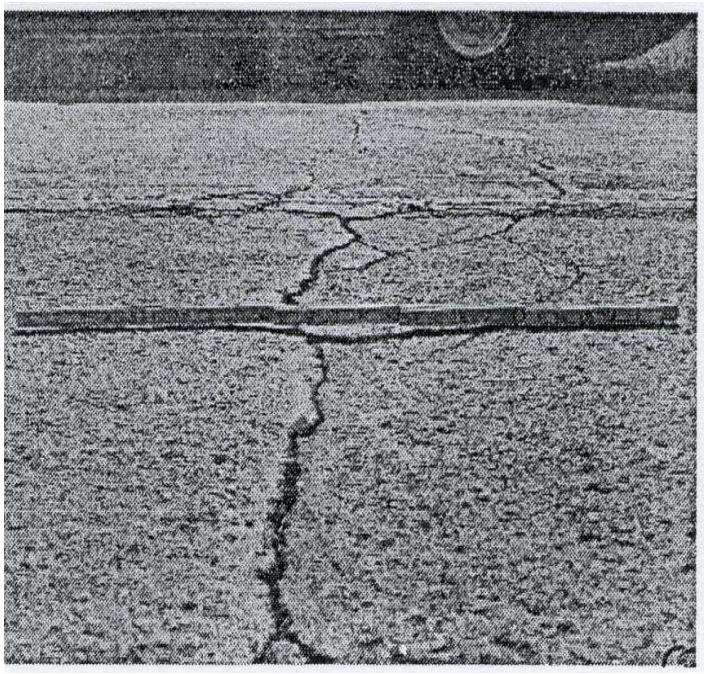

Figure 2.5: A Code 3 transverse crack

cracks. Examples of longitudinal cracks are indicated in figure 2.7. The requirement for a longitudinal crack to be considered significant is that it should lie in the wheel path, i.e., the portion of the pavement where the wheels of vehicles predominantly travel.

2.2.2 Block cracks

Block cracks comprise of rectangular blocks of interconnected transverse and longitudinal cracks. For example, the images presented in figure 2.8 indicate typical block cracking (courtesy : Google images).

The detection of such cracks can be achieved using the algorithm presented in the thesis easily enough. Whereas, the classification requires identifying the fact that the cracks present are interconnected. This might require some additional loop

Figure 2.6: Another type of Code 3 transverse crack

detecting algorithms or the presence of multiple transverse and longitudinal cracks can be assumed to represent a block crack.

2.2.3 Fatigue cracks

Fatigue cracks, also known as Alligator cracks are very finely developed patterns that appear as secondary cracking stemming from longitudinal/transverse cracking. These occur as a result of excessive loading and a weakening of the structure beneath the surface. Hence, the cracking described earlier are predominantly surface phenomena while fatigue cracks indicate the beginning of structural damage. Such cracks comprise of finely interconnected web-like cracking that resemble an alligator's hide. Hence the name alligator crack is associated with this type of cracking. Examples of fatigue cracking are presented in figure 2.9. These cracks differ from block cracks

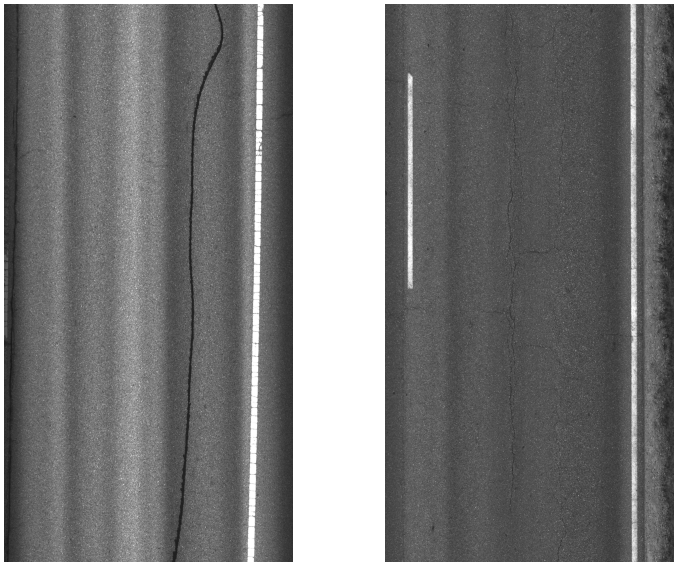

(a) (b)

Figure 2.7: Longitudinal cracks

because of the higher fineness of interconnection.

In order to detect fatigue cracking, the processing must be done at lower resolutions. That is, while considering features within subimages of a test image, the size of the subimages may have to be as small as 8×8 pixels, while a larger size of 32×32 pixels has been determined to be appropriate in the developed algorithm for detecting transverse and longitudinal cracking. Since, the fine cracks are also interconnected, again loop-detection algorithms might accurately detect and classify such cracks.

In the following section, the data collection vehicle and the associated equipment are presented. A brief description of the technique used by KDOT to record observations on cracking types and the location of cracks on highways is also presented.

Figure 2.8: Block cracks

2.3 Measurement system

In this section, we present the measurement system and techniques that have been used by KDOT to generate images of pavements and the left and right profile data for each image. Longitudinal profile data or height profiles of cracks indicate the amount of structural damage related to the crack [18]. These are applied in determining the roughness characteristics of the pavement and hence the effect on ride quality.

2.3.1 The Data collection vehicle

In this section, the data collection vehicle driven along highways to capture pavement images and profile data is briefly introduced [19].

An International Cybernetics Corporation(ICC) imaging vehicle that collects real-time high-resolution digital pavement images in all lighting conditions is

Figure 2.9: Fatigue/Alligator crack

used to map pavements at driving speeds. Quality images can be collected at speeds up to 70 mph. The vehicles consist of (1) a pavement camera(downward) system, (2) rack mounted computers, (3) laser sensors, (4) pavement lighting systems, and (5) Global Positioning System. The forward cameras, focussing on the pavement in front of the vehicle, are DVC-1310c digital video cameras with a progressively scanned image format. The downward cameras, mounted in the rear and focussing down on the road surface, are high performance, high-resolution Basler L103 line-scan cameras. Sign cameras are focussed on the side of the road for right of way analysis. The forward and line scan camera computers comprise of 3.0 GHz Pentium IV processors working on Windows 2000 with additional software that synchronize the cameras and lighting. The lighting system consists of ten 150 Watt lamps, each of which has a polished reflector designed for efficient operation. Laser sensors located on the front

bumper record the pavement elevation data, generating pavement profiles. The image data recorded using this system is saved on removable hard drives for further analysis. The information about the data collection equipment was provided by KDOT [20].

The data collection system plays an important role in this application since factors such as lighting on the pavement, position of the cameras and so on affect the quality of images used in further processing. Artificially introduced artifacts such as non-uniform lighting in images are some of the effects that have to be accounted for by image processing algorithms. Hence, the more accurate the data collection, the less complex the processing algorithms have to be.

2.3.2 Recording of crack classification

The technique currently used by KDOT to classify observed cracks on highways is based on the decision of an expert. An operator on the vehicle controls the processing of the camera-computer system. Every time a crack is observed in the image of the current section of highway, it is classified visually and the observation is recorded on a computer log. Hence, the vehicle is driven at speeds lower than highway speeds near the shoulder of the lane. This method of data recording could lead to inconsistent classification since a vast amount of data is processed very quickly. The decisions can be expected to be strife with human errors that tend to occur. Instead, if an automatic detection and classification system is implemented, the stored images could be processed in real-time or off line without human intervention. Such a system would avoid inconsistencies and save manual labor.

At present, though, pre-classified images and the profile data are provided for this research. The decision of the algorithm is compared with expert decisions to determine the accuracy of the algorithm. In later chapters, we present findings on the performance of the algorithm, which is found to be extremely accurate for transverse cracks.

2.4 Summary

In this chapter, we described the types of cracking generally observed on pavements, along with image examples. We also made observations on key features of each type of cracking that can be exploited to detect and classify them. In the final section, we presented a description of the data collection vehicle utilized by KDOT to capture pavement condition data. The technique of manual observation and classification is explained in Section 2.3. In the next Chapter, we present the first stage of the algorithm, i.e., the detection/preprocessing of pixels. This stage classifies pixels as cracked/non-cracked and filters out the pixels that are unconnected to other cracked pixels.

Chapter 3

Detection/preprocessing of cracked pixels

This chapter deals with the detection of cracks that appear in the pavement images. Pixel-level classification is performed in this stage, i.e., pixels are classified as cracked/non-cracked. The stages of preprocessing used to remove noise from the pavement image and detect connected sets of pixels that persist after noise removal are described in this chapter. We begin by presenting a brief introduction to images and how they are processed.

3.1 A brief introduction to the world of pixels and images

An image is a $2-D$ digital representation of a scene captured from light reflecting off of the subject. The smallest unit of an image is the picture element or *pixel* [21]. A pixel can be thought of as a uniform square containing some definite value of intensity or color. A number of pixels are assembled together like the pieces of a jigsaw puzzle to create a whole image. The resolution of the image is commonly such that, individual pixels are not visible as discrete squares but the complete image contains smooth gradients of color intensities. When there are objects within an image with

sudden change in pixel values from the neighboring pixels, these appear as edges.

Image processing is a vast field with applications in various areas such as transportation, medicine, military surveillance and so on. It involves extracting meaningful information from images by applying certain processes to them [22]. Though a lot of techniques are generic, some algorithms are customized depending on the application and the type of images that have to be processed. Image processing is, in fact, a branch of signal processing in which the input is an image. A detailed discussion on image processing algorithms can be found in [23].

Pavement images consist of a smooth consistent background. When cracks are present, these appear as a string of lower intensity pixels (darker than the pavement surface). Hence, the main characteristic of cracks exploited to detect them is their lower pixel intensities compared to the background pixels. In our algorithm, this feature is used in the preliminary step of thresholding as described in the following section.

Throughout this discussion, the size of the images are uniform and are 3344 × 2048 pixels (6.44m×3.94m). Each pixel is 1.93mm×1.93mm in the images. The size of the images becomes relevant when computational complexity of processing them is to be considered.

3.2 Steps involved in the detection of pixels

The processes used to achieve noise reduction and detection of connected pixels are:

Thresholding

Thresholding has been used widely as a basic technique for segmentation of the foreground from the background, noise removal, as well as image equalization [24] [25]. Generally, setting the threshold is a vital step before further processing since, using

appropriate thresholds, the noise from the image can be reduced to a great extent. In our process, thresholding is used to classify pixels as cracked or non-cracked. Here, the local statistics, i.e., mean and variance along every column and sets of rows from the image, taken one at a time, are determined. Each pixel within this block of few rows and all columns is classified as cracked/non-cracked based on a threshold corresponding to

$$T = \mu - \sigma \tag{3.1}$$

where μ is the local mean and σ is the local standard deviation. Denoting the pixel value at location (x, y) in the image as $p(x, y)$,

$$p(x,y) = \begin{cases} 1 & \text{cracked if } p(x,y) < T \\ 0 & \text{non-cracked if } p(x,y) > T \end{cases}. \tag{3.2}$$

Here is where the typical characteristic of cracked pixels having lower intensities than the background is utilized. The motivation for using a block statistic is to overcome any localized image artifact. Thus, an adaptive thresholding technique is used as the first stage of crack identification. As a result, the problem of misclassification with a single global threshold set for an entire image is avoided as well. An image with a sealed transverse crack is shown in Figure 3.1 and the result of thresholding it is shown in Figure 3.2.

In figure 3.2, a light band is seen around the crack, the cause of which is explained as follows. The processing and rendering of the image in the document cause a variety of image artifacts. When viewed on a display, the background area away from the crack, consists of highly uncorrelated pixels without an organized pattern. In the rendered image, many of the pixels coming through the threshold appear to be touching but in reality they are not. Another effect that appears in the rendered image is the light band around the crack. This band is caused by the adaptive threshold applied to the image, and is not a rendering effect. As the algorithm gets near the

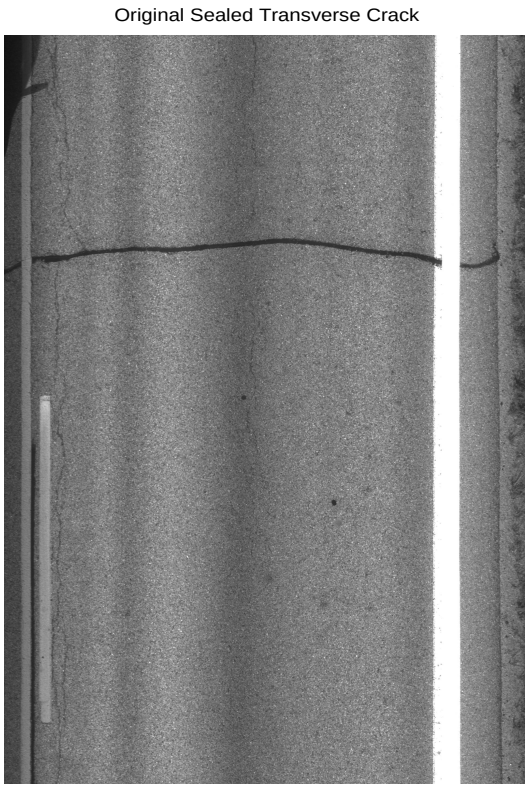

Figure 3.1: Original Image

crack the low pixel values of the crack pixels drive the threshold lower, causing fewer pixels to come through, thus creating the light band seen in the image.

3.2.1 Line Detection

Line detection denotes the process of searching for connected pixels that represent lines in the image within a certain range in the horizontal, vertical and diagonal directions. Since cracks consist of short linear segments, this range is fixed as 5 pixels, a small fraction of the subimage length to be used later in the recognition process. This process eliminates much of the clutter that resulted from thresholding the image. The larger the range within which connected sections are searched for, the more connected the image becomes but in the case of slight cracks having smaller

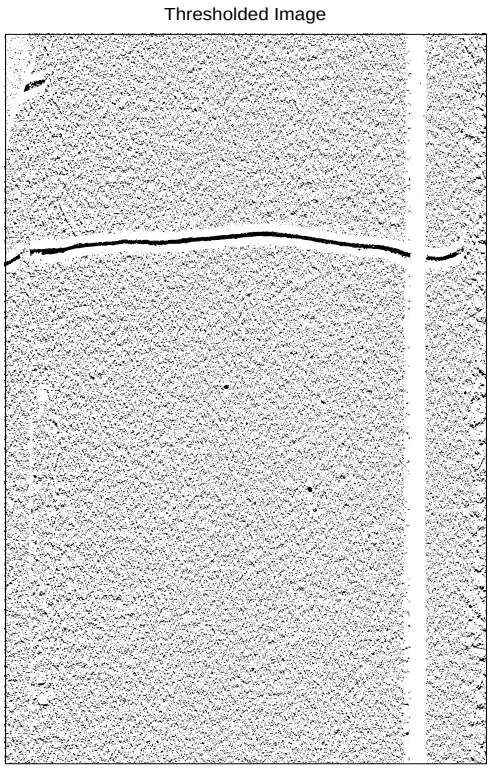

Figure 3.2: Thresholded Image

connected segments, larger ranges could miss these cracked portions. Hence a tradeoff is required to find the optimal range. We determined that choosing 5 pixels was appropriate to preserve maximum possible information about the cracked portions in the image. The process of searching for connected pixels is repeated in the horizontal, vertical and diagonal directions for each cracked pixel. This accounts for all possible directions in which a crack could extend. Upon line detection the thresholded image in Figure 3.2 is transformed as shown in Figure 3.3.

From Figure 3.3, it is observed that the process of line detection causes a filtering effect by retaining only connected pixels. Hence, the number of noisy pixels is reduced in the image after line detection. There are, however, a large number of noisy pixels which need to be filtered out to avoid false detection in the final stages

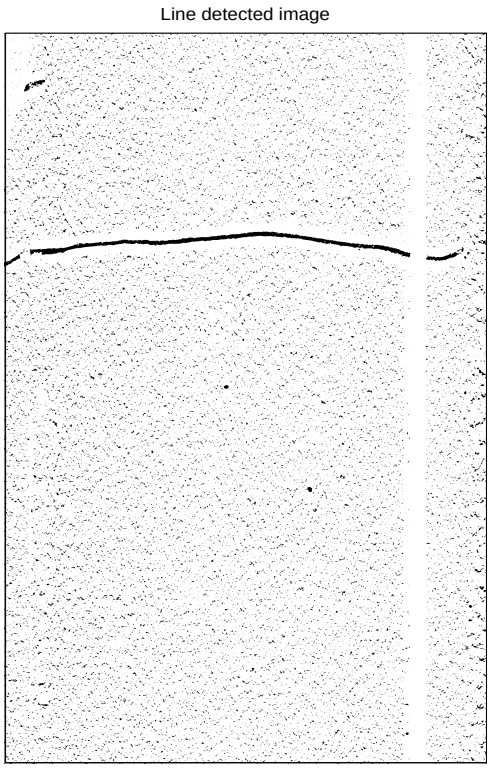

Figure 3.3: Line detected Image

of the algorithm.

3.3 Summary

In this chapter, we have described the basic preprocessing performed on an image to remove most of the background noise and preserve only the connected cracked pixels. The efficiency of this stage is critical to the subsequent stages since the presence of a large amount of clutter would affect the higher levels of classification. It is noteworthy that the pixel detection algorithm presented in this chapter works very well to attain the objective of determining cracked pixels that are connected to other cracked pixels. The next chapter presents the stage of subimage level classification used to further

reduce the number of noisy pixels.

Chapter 4

Recognition of cracked subimages

This chapter deals with classification at the subimage level, i.e., recognition or validation of the subimages that contain some portion of cracked pixels. In this stage, the image is divided into subimages of size 32×32 pixels. This division reduces the complexity of further processing. The size of the subimage is chosen such that it sufficiently characterizes the complete crack as well as reducing processing time. The steps involved in classifying the subimages and the basic concepts that have been applied are presented in the following sections.

4.1 Grouping of cracked pixels

The classified pixels are grouped into subimages of size 32×32. Next, each subimage is classified as cracked or non-cracked based on the number of cracked pixels in it. We set our decision threshold to 10%, i.e., if 10% or more of the pixels in a subimage are cracked, the subimage is classified as cracked. The purpose of grouping is to restrict all further processing to the subimages so as to reduce computational complexity. Furthermore, when characterizing cracks as sealed/unsealed (Section 6.2), this characterization is made based on classification of subimages as sealed/unsealed. Therefore, only by grouping pixels into subimages can this classification be performed

at the subimage level. Grouping pixels into subimages has been applied previously in [26]. In this paper, though, the subimage size used was 64×64 pixels. The high rate of false object detection (0.79) per image frame indicates that the algorithm is not very efficient. It is observed that the subimage size of 32×32 sufficiently captures cracking information from the image. A smaller size, such as 8×8, leads to slower processing, which can be avoided when there is no fine cracking. A larger size was found unsuitable since portions of cracks were incompletely traced, thereby causing loss of data.

4.2 Recognition using Principal Component Analysis(PCA)

In this section, we present a discussion of the technique used to extract features that can distinguish cracked and non-cracked images. A brief explanation of PCA is provided and its application to pavement cracking is substantiated with image results.

4.2.1 Principal Component Analysis

In the recognition phase of the algorithm, the 32×32 subimage classification is further refined using PCA based feature extraction. PCA is a statistical technique used to reduce the dimensionality of data. The principal components extracted from a given data set are determined such that they represent as much of the variation in the data as possible without considering all the points in the set. A description of this technique is found in [27]. In [28], the authors propose the application of PCA to enhance open cracks that occur on severe metallic surfaces. PCA has been used for thermal effect enhancement while processing thermographical images of metallic surfaces for open cracks. This is one possible application of PCA, which is a very commonly used effective data processing technique. In our application, we propose the use of PCA to extract principal features that could distinguish cracked sections

of an image from non-cracked sections.

4.2.2 Application of PCA on images

PCA is initially performed on a set of 50 concatenated non-cracked images, and three basis vectors corresponding to the first three principal components are extracted. The first three components constitute our feature set as they capture around $96 - 97\%$ of the information in an image and can be used to adequately characterize the entire image. Following the extraction process, we populate two training classes of cracked and non-cracked subimages from 50 cracked and non-cracked images. Each cracked subimage is projected onto the basis vectors and three weights, w_1, w_2 and w_3, are extracted. These weights indicate the amount of energy present in each of the principal component directions in the vector space defined by the basis vectors. This process is repeated for all the collected cracked subimages. Simultaneously, the same process is performed on the collection of non-cracked subimages as well to obtain weights for the class of non-cracked images. The number of subimages in each class is increased by testing more images and hence, more weights are appended to the classes. There are six distributions of weights totally, and each can be characterized using the probability density functions. As per central limit theorem, the weight distributions are observed to be normal with different means and variances [29]. In order to test a subimage for the presence of a crack, its three weights, w_i, $i = 1, 2, 3$, are obtained by projecting the mean subtracted subimage onto the bases vectors computed earlier. Each of these three weights are compared to two distributions - $w_{c,i}$ distribution for the cracked class and $w_{uc,i}$ for the non-cracked class. The probability of the test subimage weights being closer to one distribution than the other is computed as a likelihood function presented in equation 4.2. This likelihood function is compared to a threshold as shown in equation 4.4 based on which the subimage is classified. Thus, a Bayes likelihood test, with the following hypotheses, is developed under the

assumption of normality [30].

$$\begin{aligned} Cracked\ H_0 &: w_i \sim N(\mu_{c,i}, \sigma^2_{c,i})\ i = 1,2,3 \\ Non-cracked\ H_1 &: w_i \sim N(\mu_{nc,i}, \sigma^2_{nc,i})\ i = 1,2,3 \end{aligned} \tag{4.1}$$

where $\mu_{c,i}$ and $\sigma_{c,i}$ are the mean and variance of weight $w_{c,i}$ for the class of cracked subimages; $\mu_{nc,i}$ and $\sigma^2_{nc,i}$ are the mean and variance of the weight $w_{nc,i}$ for the class of non-cracked subimages. The likelihood ratio based on weight w_i is formulated as

$$L(w_i) = 0.5 \log \frac{\sigma^2_{c,i}}{\sigma^2_{nc,i}} + \frac{(w_i - \mu_{c,i})^2}{2\sigma^2_{c,i}} - \frac{(w_i - \mu_{nc,i})^2}{2\sigma^2_{nc,i}} \tag{4.2}$$

where $i = 1, 2, 3$. Assuming a uniform cost function and defining the threshold τ as

$$\tau = \frac{P_c}{P_{nc}}, \tag{4.3}$$

where P_c and P_{nc} are the prior probabilities of a subimage being cracked or non-cracked respectively, the Bayes test is given by

$$\delta(w_i) = \begin{cases} 1 & L(w_i) > \tau \\ 0 & L(w_i) \leq \tau \end{cases}. \tag{4.4}$$

Thus a value of 1 for $\delta(w_i)$ indicates a cracked subimage while 0 indicates a non-cracked subimage. The prior probabilities P_c and P_{nc} are evaluated based on existing data on pavement distress. In our analysis, we determine that $P_c = 0.0435$ and $P_{nc} = 0.9565$.

4.2.3 Decision via sensor fusion

The decisions based on the three weights i.e. the results of the Bayes test for $i = 1, 2$ and 3 are fused using the OR rule and a combined decision is used to classify the subimage. Thus, a sensor fusion like approach is applied to validate the decision of the classifier. Sensor fusion is a technique applied to enhance the reliability of the

output or decision of one sensor. Decisions reported by multiple sensors which work independently can be fused to make the result more accurate than the output of one sensor [31]. In this research, the decisions of the classifier based on each of the three weight features are treated as independent sensor decisions and fused so as to obtain a better classification of subimages. It is visually observed that this type of fusion results in a nearly complete crack compared to when one of the weights is used. In the latter case, a lot of cracked subimages get filtered and the crack appears incomplete in parts.

4.3 Image results

The image obtained after recognition is presented in figure 4.1.

Blocks of size 32×32 are observed to constitute the crack in the recognized image. The number of classified subimages is much lower than what was detected. Thus, noise reduction occurs in this stage as well. It is evident from the image that, the chosen subimage size is appropriate for characterizing cracks present. This claim is further substantiated in Section 6.4 by presenting an example of an unsealed crack that has been processed.

4.4 Summary

In this section, the process of grouping pixels into subimages to reduce computational complexity has been presented. We also describe Principal Component Analysis as applied in feature extraction for distinguishing cracked and non-cracked images. Following this section, a brief discussion on classification of subimages via sensor fusion is presented. Finally, the image resulting from the application of PCA based recognition is shown and observations are presented. In the next chapter, postprocessing performed on the recognized images is described.

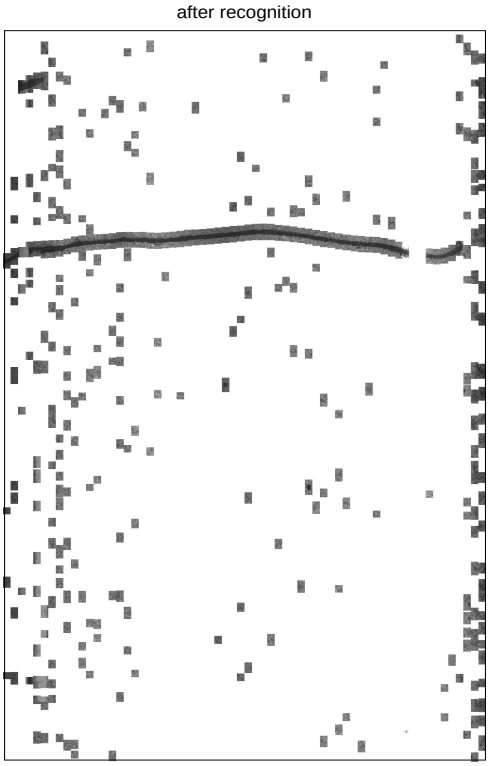

Figure 4.1: Image after the recognition stage

Chapter 5

Postprocessing

In the previous chapter, the third stage of the algorithm, i.e., recognition of subimages, was presented. The image after recognition is comprised of square blocks or subimages. For any cracks present, subimages constituting the cracks are clearly observed. There are certain cases of mild cracking in which the cracked subimages are not completely connected. Moreover, there are cases of isolated non-cracked subimages throughout the image as observed in the figure presented in Section 4.3. Hence, postprocessing is performed on the recognized image to establish subimage connectivity and filter out isolated subimages. This stage is comprised of two processes : application of mathematical morphology and filtering.

5.1 Mathematical Morphology

Morphology, or the science of shape, has been applied in image processing very extensively. Specifically, this technique has been applied in areas such as image enhancement, feature extraction and object recognition [32] [33]. With primary focus on binary images, morphology deals with representing objects in an image in more useful forms. A variety of filtering effects can be created from combinations of different morphological operations. In simple terms, morphology involves filtering an

image with a suitable structural element that is sequentially placed over every pixel in the image. Structural elements can be linear, circular or any other shape depending on the objects to be recognized or enhanced. In [34], the authors have applied morphology as part of an image processing algorithm to detect cracks. Several other similar research efforts have included morphology as the final stage before presenting the resultant image to the end user. This extensive usage of morphology indicates its effectiveness in relevant applications. Since pavement distress detection can be treated as an image enhancement problem, morphology can be applied to cracked images to efficiently segment the cracks and eliminate clutter and pavement noise.

There are two basic morphological operations, namely dilation and erosion, that can be employed to enhance the objects in an image. Dilation is the process of removing small holes while erosion is the process of removing small objects. Image dilation causes subimages to get elongated and hence connection is established between subimages that are not adjacent but are part of the same crack. Then, by eroding this image, objects are compressed to their original size but the previously established connection is maintained. A closing operation (dilation followed by erosion) is thus used to enhance the objects in the image, i.e., distresses such as cracks in this case. As expected, it is observed that slight cracks appear better connected after the application of the above processes. Furthermore, a large number of isolated subimages that were retained till this stage are removed from the image by the application of morphological closing.

The choice of the structural element is an important factor to be considered while dilating or eroding an image because the shape of the objects in the image could get distorted by the application of the wrong type of structuring element. Since pavement cracks are made up of linear segments, linear structuring elements are used to perform a closing operation on the image. A 4-pixel wide horizontal line filter is used to close the image. In parallel, another line filter, vertical and 4 pixels

long, is applied to detect any longitudinal aberrations in the image. Once again, the choice of pixel length was based on our experience from analyzing actual images by applying morphology. When the pixel length is set at 3 or lower, connectivity is lost in several sections of a crack. On the other hand, for a pixel length of 5 or greater, several isolated non-cracked subimages were artificially connected, presenting false information. The pixel length of 4 connects up adjacent cracked subimages well enough for a crack to be recognized while avoiding spurious connections between isolated subimages.

The image that results upon dilation of the original image is presented in Figure 5.1 and the result of erosion on the dilated image is shown in Figure 5.2.

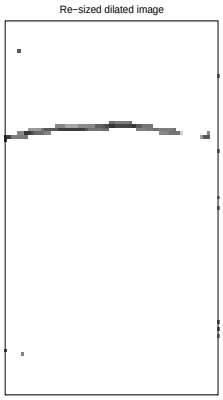

Figure 5.1: Image after Dilation

Generally, morphological operations are applied at the pixel level. Moreover, for large images, the operations tend to become computationally very intense. Hence, the image being tested is resized so as to represent each subimage by one pixel. As a

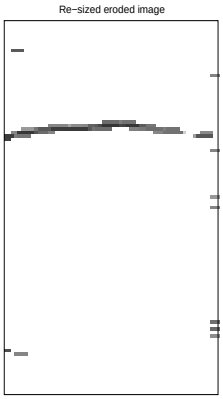

Figure 5.2: Image after Erosion

result, the size of the image used in this stage is 105×64 pixels. After postprocessing the image, it is again re-sized to its original dimensions. Following morphology, a final filter is applied to the image to remove isolated subimages. The design of this filter is presented in the following section.

5.2 Filtering

The postprocessed image consists of fewer isolated subimages than the image immediately after recognition. The persistence of such subimages is due to clustered sets of non-cracked subimages consisting of some anomalous surface phenomenon which might have been detected as a crack. In spite of the reduction in the number of falsely detected subimages, a more precise image is desired in order to avoid false localization of cracks within the whole image. Hence, a final filtering process is performed

on the image. The design of this filter is based on the simple idea that any detected subimage that is not surrounded by any other detected subimage within a certain radius in all directions around it is considered isolated enough to be eliminated. The radius is heuristically determined to be thrice the length of a subimage and it has been found to perform well in eliminating isolated subimages.

5.3 Image results

Upon postprocessing, the resulting image appears as shown in Figure 5.3. As observed in the image, there are very few isolated subimages that are retained after postprocessing. However, even a few subimages that are oriented across a single row could affect the detection of a cracked row in the next stage where the cracked subimage count is used to classify the whole image as cracked or non-cracked. This problem is explained further in Section 6.1.

5.4 Summary

In this chapter, we presented the stage of postprocessing applied to the image after recognition of the cracked subimages. Most of the isolated subimages were efficiently eliminated while connectivity is established between subimages constituting the actual crack. The final filtering process further reduced the remaining isolated subimages in order to avoid false crack localization in the next stage of image level classification. In the next chapter, the feature used to identify the precise locations of cracks within the image is presented. In addition, the performance of this feature in classifying whole images is indicated. Also presented in this chapter is the application of a Fourier based technique to classify cracks as sealed or unsealed, which determines maintenance requirements for the cracks.

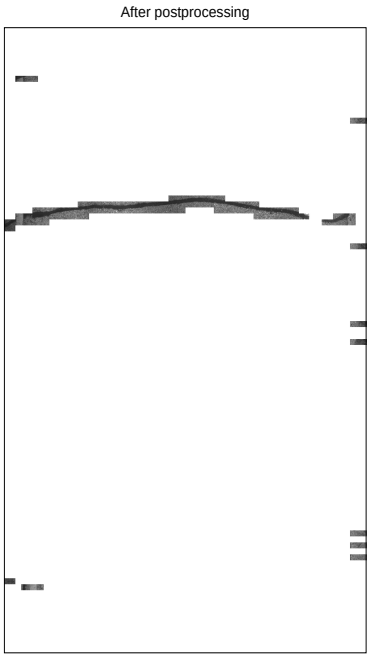

Figure 5.3: Image after Postprocessing

Chapter 6

Image classification, crack counting, visualization and large-scale testing results

In the previous chapter, we described the third stage in the algorithm, i.e., postprocessing performed to establish connectivity among cracked subimages and to eliminate isolated noncracked subimages. In this chapter, the algorithm progresses to image level classification. In this stage, the number and orientation of cracked subimages are exploited. These characteristics are used to classify the whole image as cracked or noncracked. Furthermore, the exact locations of cracks within the image are identified and highlighted for better visualization. As a result, the number of cracks present is also determined automatically by the algorithm. The most important contribution of this stage is the sub-classification of cracks as sealed or unsealed using a Fourier transform based approach. Further explanation on this nature of the subimage and its significance is provided in Section 6.2. In closing, large-scale testing conducted on the complete algorithm is presented. The results observed along with the probabilities of detection and false alarms are presented to validate the

performance of the algorithm.

6.1 Image classification

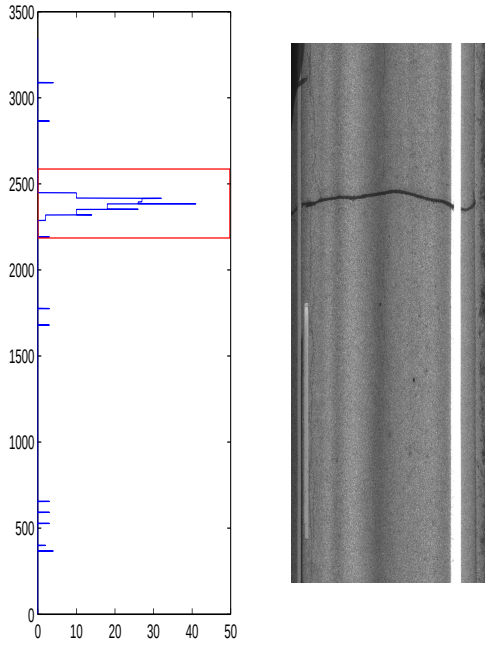

Figure 6.1: Original image with its subimage profile

In order to localize the cracks within an image, the number of cracked subimages per row and per column are determined and plotted. The subimage profile developed for the transverse crack under consideration is shown in figure 6.1. In the plot shown, the $y - axis$ represents the row number and $x - axis$ represents the subimage count. This count of cracked subimages is termed as subimage profile, not to be confused with pavement profiles that indicate elevation nature of pavements. The steep increase in the subimage profile in the plots indicates the presence of cracks. This feature can be exploited to further localize the crack and present it to the user. Comparing this count to the average score of the image with a tolerance

of 2 $\times$ standard deviation indicates the location of the crack. By considering either the whole image or subbands of the image, multiple cracks, in either direction, can be detected. By tracking the number of occurrences of the subimage profile exceeding the threshold, the total number of cracks that occur in an image is determined. Hence, this level of classification is of very low complexity from a computation standpoint. The importance of presenting a clutter free image to this stage should be noted. When there are falsely detected subimages present, they shift the statistics of the subimage profile. As a result, the rows around which these false alarms occur could also be identified as containing parts of cracks leading to false classification. Hence, the number of isolated noncracked subimages needs to be restricted before this stage. A few cases of isolated subimages do not affect the threshold greatly since it is dominated by actual cracked subimages which exceed isolated subimages significantly. The feature of subimage profile is observed to detect cracked rows/columns within images highly efficiently. Hence, the classification of whole images is accurate as well.

From a visualization standpoint, the ability to highlight a crack is useful for the end analyst. Therefore, while displaying the images we have consciously represented the cracks against a white background. Integrating the location of cracks with a mapping software can provide valuable information for maintenance activities.

6.2 Classifying sealed and unsealed cracks

When a region within an image is determined to contain a crack, the cracked subimages in this region are tested to determine if the crack is sealed or unsealed. Sealed cracks are those cracks to which sealants have been applied so as to control the rate of their growth and the pavement roughness caused by serious cracking. Hence, sealed cracks do not represent an immediate threat to pavement health whereas unsealed

cracks, specifically ones that extend across the width of the pavement require attention.

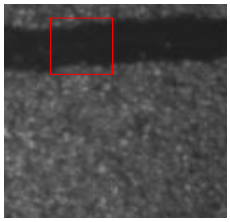

Figure 6.2: Sealed subimage

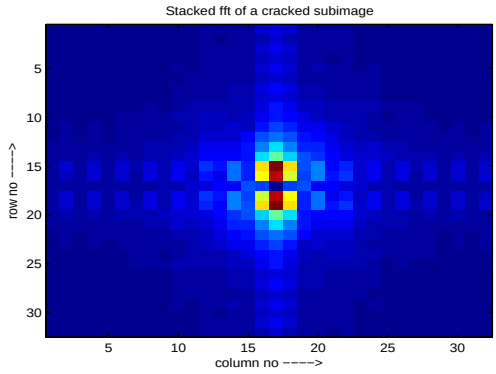

Figure 6.3: FFT of a subimage with a sealed crack

The application of sealants makes cracks wider than unsealed cracks, also making them very distinct and easier to detect. From visual observation of samples of both types of cracks, it is intuitive that the frequency response of each must be different. This is to be expected since a sealed crack is very distinct from the pavement surface and hence there is a large intensity gradient at the crack edges. In comparison, there is little or no distinction between unsealed cracks and the pavement surface. Hence the frequency response of unsealed cracks are expected to resemble that of the

noncracked pavement more closely than the response of sealed cracks. Therefore, the frequency characteristic of a crack is a possible measure of classifying it. To extract the frequency content of subimages, we perform $2-D$ Fourier transform on them. The FFT of various 8×8 portions of each test subimage are computed and their magnitudes are stacked. The frequency response resulting from the stacking has a distinct shape indicating the orientation of the crack within the subimage. This technique of stacking up the magnitudes of the FFTs has been previously applied [35] to analyze quality of baked products. The stacked magnitudes of the frequency responses have an expected value which is a scaled version of the frequency response of the subimage. This has been proven mathematically in [35]. If the Fourier transform of the 32×32 subimage is represented as $S_{32\times32}$ and that of the 8×8 subimage as $S_{8\times8}$,

$$\mathrm{E}\{|\mathrm{S}_{8\times8}(x,y)|^2\} = |\mathrm{S}_{32\times32}(x,y)|^2\, N \tag{6.1}$$

where N is the number of 8×8 subimages within one 32×32 subimage.

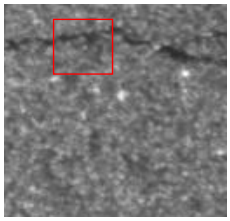

Figure 6.4: Unsealed subimage

Equation 6.1 indicates that the summed magnitudes of FFTs from identical 8×8 portions of a subimage serve to emphasize the dominant features in the subimage representing a crack.

Figures 6.2 and 6.4 present an area around sealed and unsealed cracked portions. Though each subimage size is as indicated by the red rectangle, for easy

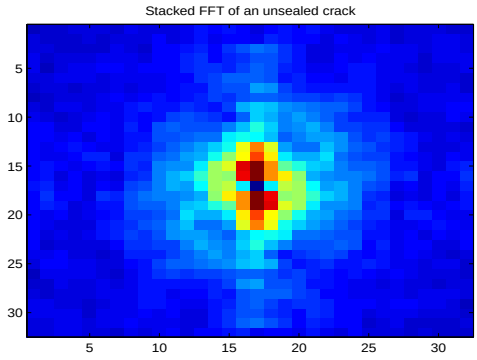

Figure 6.5: FFT of a subimage with an unsealed crack

visualization, a larger area has been presented. Figures 6.3 and 6.5 present the image representation of the Fourier transform of a subimage from the sealed and unsealed cracks respectively. From figure 6.3, it is seen that sealed cracks exhibit a narrow response while unsealed cracks have a greater spread in their response. A measure that characterizes the spread can serve as the feature to distinguish between sealed and unsealed cracks. Specifically, the number of significant frequency components, K_{w_f}, in the spatial domain is used as an indication of the spread in the FFT. In practice, frequencies having magnitudes greater than 20% of the maximum frequency are considered significant in the frequency response of a subimage. Computing this feature for a large number of subimages yields a normal distribution for each class with different means and identical variances, i.e., $N(\mu_{\text{sealed}}, \sigma_{\text{s}}^2)$ and $N(\mu_{\text{unsealed}}, \sigma_{\text{s}}^2)$. For a test subimage, the number of significant frequency components are determined and compared to the means of the two classes. The resulting decision is similar to the Gaussian location testing rule and can be represented as

$$\delta(K_{w_f}) = \begin{cases} \text{sealed} & \text{d}(K_{w_f}, \mu_{\text{sealed}}) < \text{d}(K_{w_f}, \mu_{\text{unsealed}}) \\ \text{unsealed} & \text{d}(K_{w_f}, \mu_{\text{unsealed}}) < \text{d}(K_{w_f}, \mu_{\text{sealed}}) \end{cases} . \tag{6.2}$$

where d indicates the distance between the metric and the means of the distributions. All the subimages within a detected region in the image are subjected to this test. If

the majority of the subimages are classified as sealed, the crack as a whole is classified as sealed. On the other hand, the crack is classified as unsealed if the majority of the subimages are classified as unsealed. With 50 test images, the proposed technique provided 100% accurate classification of sealed and unsealed cracks.

6.3 Large scale tests

- The term 'large scale' is used to indicate that a sequence of images have been processed sequentially by the algorithm which retrieves images automatically from the database. A set of 1000 images that contain transverse cracks ranging from severe to mild have been processed by the algorithm. This set also consists of some noncracked images. It is observed that the algorithm has a high rate of crack detection with a low false alarm rate. Specifically, the probability of detection of cracks is found to be 0.9710 and the probability of false alarm is found to be 0.0076. One key observation is that even multiple cracks within an image are detected accurately. However, in some cases of mild cracks that do not run across the width of the image, there is a possibility that the crack goes undetected. But, as is evident from the remarkably high rate of detection, such occurrences are rare.

- As far as longitudinal cracks are concerned, around 34 images containing longitudinal cracks were tested. The probability of detection was found to be 0.9411. However, there were more false alarms compared to transverse crack testing. A higher false alarm rate of 0.20 is induced by artifacts such as lightning stripes and surface characteristics. Distinguishing such clutter from relevant cracking will require a more complicated detection algorithm as compared to transverse crack detection.

- In the case of very mild cracks, there is a chance of misclassification since these

might be interpreted as non-cracked portions in the image. The large set of images contains pavements with different types of surfaces, with varying degrees of texture. The more texture the pavement surface has, the more chances of misclassification since slight cracks are difficult to distinguish from such backgrounds.

- The accuracy of sealed-unsealed crack classification is found to be 100% in the 50 test images considered. There is a small probability of misclassifying non-cracked images as sealed images when there is non-uniform lighting, such as shadows or dark stripes in the image. Also, some sealed cracks that are thin may get misclassified as unsealed cracking. But the probability of these occurrences is expected to be tolerable.

6.4 Image Examples

An example of an unsealed transverse crack is shown in figure 6.6. The results of applying the detection algorithm on this image are indicated in figures 6.7, 6.8 and 6.9. It is observed that despite the crack appearing to be slight against the pavement surface, the algorithm detects and localizes it accurately indicating the algorithm's robustness.

Examples of images containing longitudinal cracks and block cracks are shown in figures 6.10 (a) and 6.11 (a) respectively. The corresponding postprocessed images are shown in 6.10 (b) and 6.11 (b).

6.5 Summary

In this chapter, the final stage, i.e., image level classification was presented. Application of the feature termed as subimage profile to determine the number of cracks within an image, their precise location and hence the nature of the whole image is

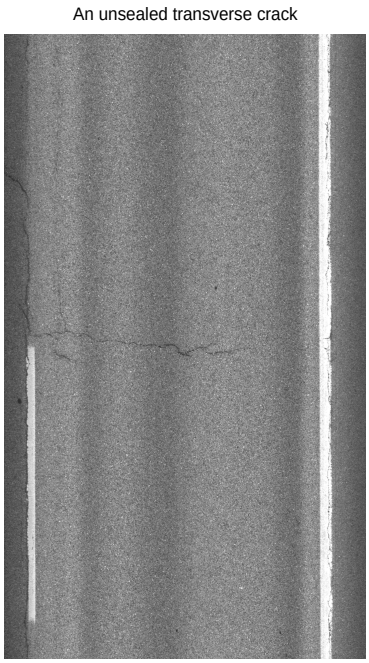

Figure 6.6: Example of an unsealed Transverse crack

presented. The most important contribution of the stage, i.e., classification of cracks as sealed or unsealed using a Fourier transform based approach that is applied at the subimage level is described in detail. Following sealed/unsealed and image level classification, the results of large scale testing of the algorithm are presented with more analyzed image examples that serve to illustrate the effectiveness of the developed algorithm. The high rate of crack detection indicates the performance accuracy of the algorithm. In the next chapter, the current research being undertaken with regard to pavement profile/elevation analysis and its integration to the results of image analysis are presented.

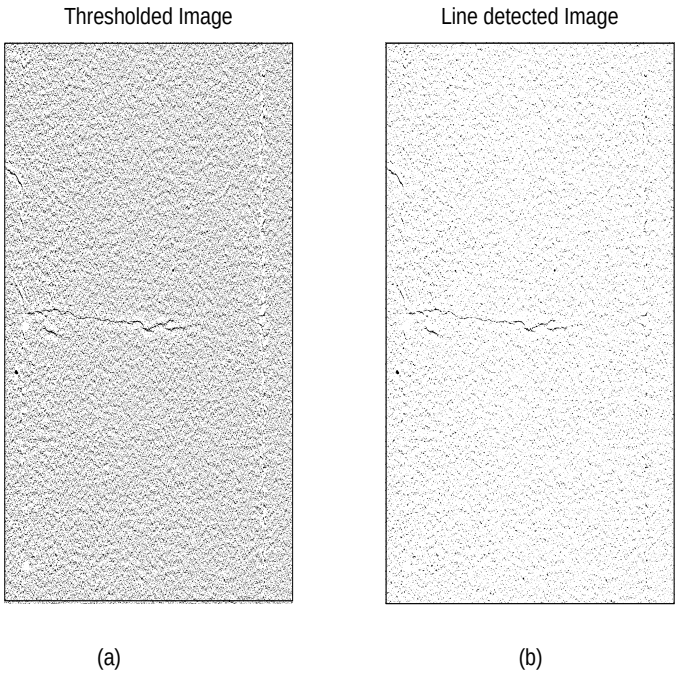

Figure 6.7: (a) Thresholded Image (b) Line detected Image

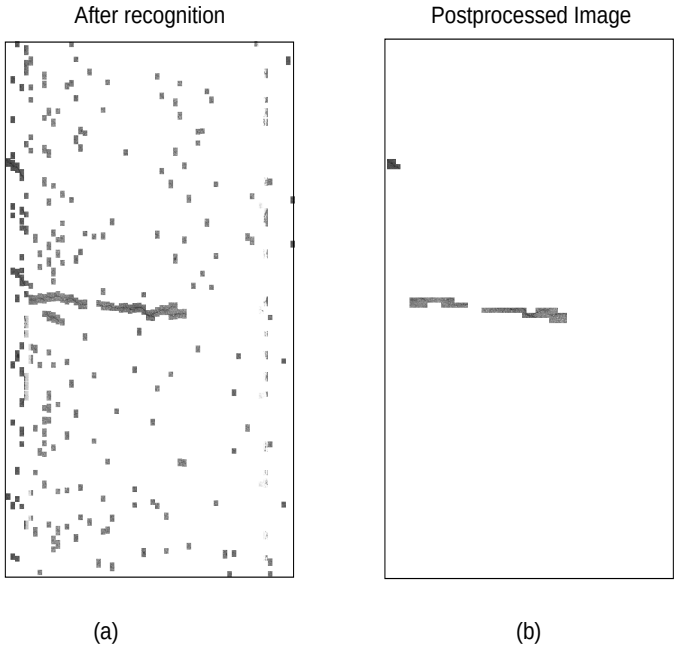

Figure 6.8: (a) Image after recognition (b) Postprocessed Image

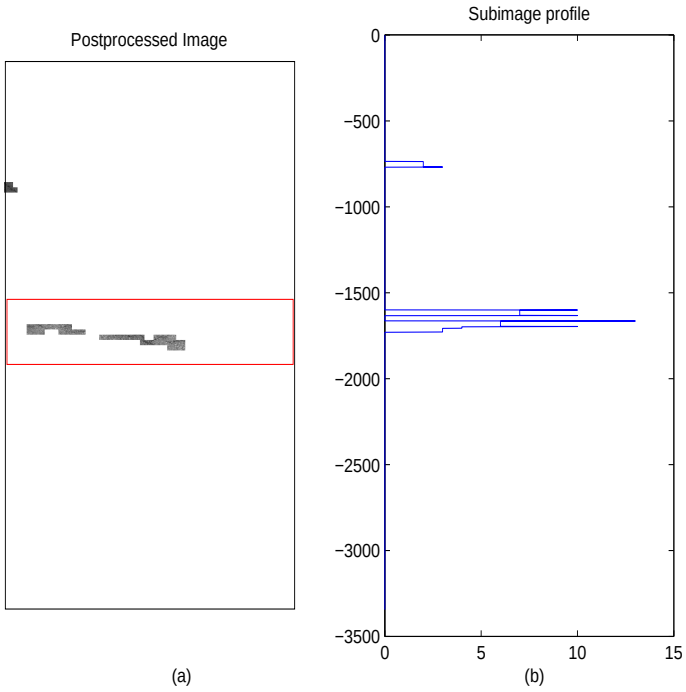

Figure 6.9: (a) Crack localization (b) Subimage profile

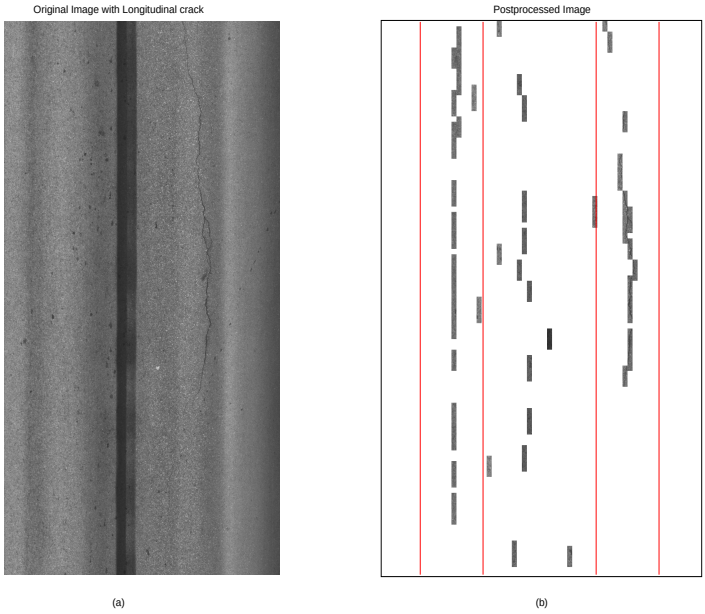

Figure 6.10: (a) Example of a Longitudinal crack (b) Postprocessed Image

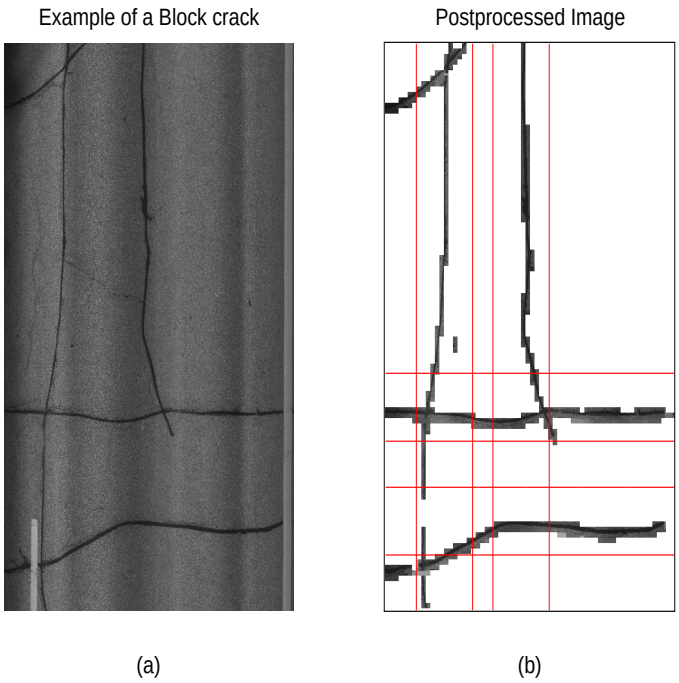

Figure 6.11: (a) Example of a Block crack (b) Postprocessed Image

Chapter 7

Pavement profile analysis and integration with image analysis

In the previous chapters, the stages involved in processing pavement images to extract relevant information about cracks were described. Following the final stage of the algorithm, large-scale testing results were also presented. This chapter deals with pavement profile characterization. The imaging vehicle that captures pavement images also records pavement profiles using accelerometers. The profile or elevation data indicate variations in depth on the pavement surface determined by a laser sensor that is directed at the pavement from the vehicle. The profile data provides useful information regarding pavement surface roughness. Cracking on pavements appear as sudden dips or peaks in the profile. Quantifying these deviations indicate the severity of cracking, based on which cracks can be classified into different codes. In this chapter, a description of profile measurement is presented, followed by extraction of cracking/roughness information from the profiles and integrating the observations with those from image analysis.

7.1 Measurement of pavement profile data

Pavement profile data are measured with the use of devices called accelerometers. These devices measure and record longitudinal profile in the left and right wheel paths. The profile data points that are measured indicate the rut depth at specific locations on the pavement. Hence, the data generated from the accelerometers comprise of two vectors of depth data measured in inches. Correspondingly, the spatial locations of the measurements are recorded as miles along the pavements. Transverse cracking on pavements manifest themselves as high frequency deviations in the slow varying profile data. The steepness of these deviations depend on the severity/degree of roughness of the cracking. The objective of this phase is to employ filtering and other feature extraction techniques that could demarcate the presence of cracks on the pavement surface. As described in Section 2.1, the profile data of a pavement section indicates variations in roughness and hence can be used to identify the code of cracking present. Classification of transverse cracks into codes $0, 1, 2$ or 3 is important to prioritize the sections of highways that are in immediate need of repair/maintenance action.

Though the depth data is presented in inches with the locations recorded in terms of miles, conversion of these values to feet/metres could help in better visualization of the phenomena in question. At other instances, the use of some automated software creates a requirement for back conversion to inches/miles. Hence, a table of unit conversions that were used in profile analysis is presented below.

Table 7.1: Unit conversions

1 mile = 5280.39 feet = 1609.344 meters
Distance between samples = 3.69×10^{-5} miles or 0.1946 feet
Number of samples per image ≈ 108
Sampling wavelength $\lambda_s = 0.1946$ feet
Sampling frequency $f_s = 5.1385$ samples/feet

7.2 Extraction of features from profile data

Observation of the profile data of large sets of images indicate that the presence of severely rough cracks causes relatively high frequency dips on the data. Some of the techniques that have been attempted to extract such deviations include wavelet analysis [36] and stochastically modeling the profile data [37]. In the following subsections, we present the various filtering techniques that were employed in order to identify significant deviations in the profile data.

7.2.1 Linear fit

In this section, we present the first technique that was identified in order to extract cracking information from profile data. A linear fitting process, which can be viewed as a rolling straight edge, was applied to the original profile. In this process, a line is constructed between the end points of a window and the deviation from the line to the profile is computed. If the maximum deviation between the line and profile is greater than a threshold, that sample is considered a defect. Now, setting the window length and threshold value are considered.

Setting the threshold as a low value yields several noisy deviations. Whereas, setting very high thresholds may result in missing deviations that might be relevant. Currently, a threshold of 0.03 is used to perform the linear fit. To determine the maximum possible deviation from a linear fit, different window lengths are applied. We apply window lengths of 8 to 10 samples, i.e. of the order of 1.56 to 1.95 feet. The window lengths also affect the linear fit. Lengths longer than 10 samples might affect several samples around the deviations while shorter lengths might miss the wide deviations. Hence, a medium window length in the range discussed is used. The profile data of a section of highway represented by around 600 images is represented as shown in figure 7.1.

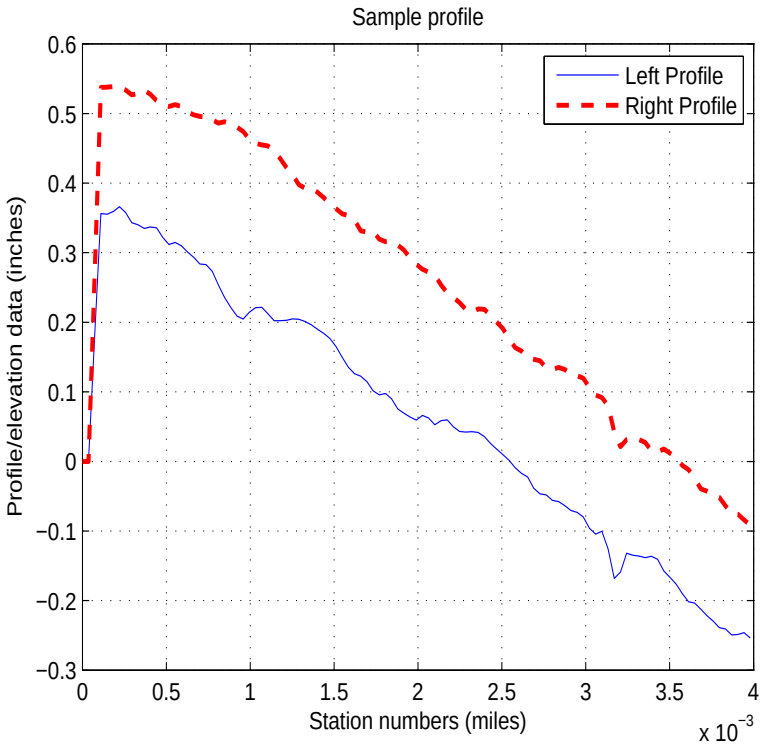

Figure 7.1: Left and right profiles of one pavement image

The profile shown in figure 7.1 captures the general characteristic of the profile data for larger sections of pavement. There is a low frequency trend that indicates pavement surface features while occasional peaks and dips indicate surface phenomena such as cracking. The linear fit algorithm performs a curve fitting that identifies the relevant deviations. The linear fit performed on the sample profile in figure 7.1 is shown in Figure 7.2.

The points of differences between the actual data and the linear fit are considered to indicate cracking on the corresponding regions in the pavement image. It is observed that there is an offset in the profile due to delayed recording on the accelerometer and hence in most cases, there is not an exact correspondence between the cracked locations determined from the profile and the image. However, deviations are observed to occur in the vicinity of the crack and hence can be matched

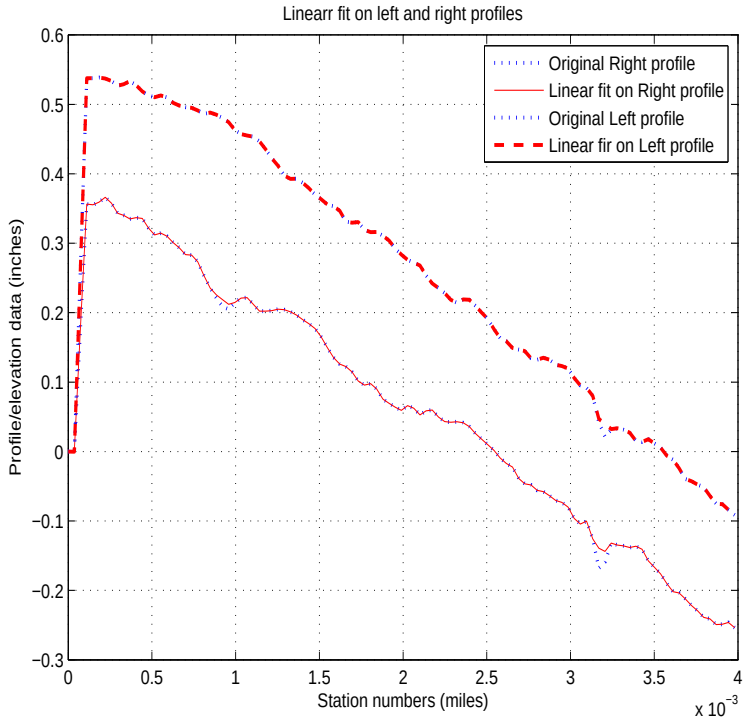

Figure 7.2: Linear fit curves

with the actual crack. In this technique, the feature extracted to identify a crack and its severity is the degree of deviation of the linear fit from the original profile data. Observation of this feature for different codes of cracks indicates that the deviations increase with increasing crack severity/roughness, with code 0 and code 1 cracks exhibiting no deviations at times. Code 3 cracks have relatively large deviations while code 2 cracks have less severe deviations. Based on these observations and the values extracted from the profile analysis, thresholds are set to distinguish the codes. Furthermore, the result of sealed/unsealed classification, from Section 6.2, is combined with the threshold-based classification to validate the code of the cracks. Due to insufficient training data, the thresholds have not been accurately characterized. Availability of more code 2 and code 3 cracks for observation could give a clearer idea of the thresholds to be set for classifying them.

This feature may be suitable only for a narrow range of pavement profiles since it is highly dependent on the window lengths which are set to be constant for all the profiles. Hence, alternate approaches are presented in the following subsections.

7.2.2 Highpass filtering

The second technique that was used to extract meaningful information from raw profile data is that of highpass filtering. A Butterworth highpass filter is designed with an appropriate cutoff frequency set in terms of wavelength. The wavelength is considered based on the mile marker rate, i.e., 0.195 feet, which indicates the distance(in miles) between the station numbers of two consecutive profile measurements. From this value, the sampling frequency is determined to be 5.14 samples/feet. The term samples is used to indicate profile data. Filters of different lengths are operated on a section of profile (covering 10 images). The filtered profiles using different cutoff wavelengths are presented in Figures 7.3, 7.4, 7.5, 7.6 and 7.7 with the filter length varying from 5 feet to 35 feet.

From figure 7.3, it is observed that the 5 foot filter does resolve the relevant deviations to some extent. However, these peaks and dips are not very distinct from the neighboring points. The application of this filter to a profile section which consists of more high frequency components may yield completely indistinguishable results. When the cutoff wavelength is increased, the number of low frequency components that begin to appear in the filtered output increases. Yet, the deviations caused by cracking appear more clearly. However, beyond 25 foot, the curve starts to appear smoother and more even, i.e., low frequency components start obscuring the deviations. Hence, an appropriate wavelength would lie in the range considered for this section of profile. But for different sections with different pavement characteristics, the wavelength appropriate for this section may not be suitable. Hence, some definite feature indicating cracking locations must be extracted from the filter output. This

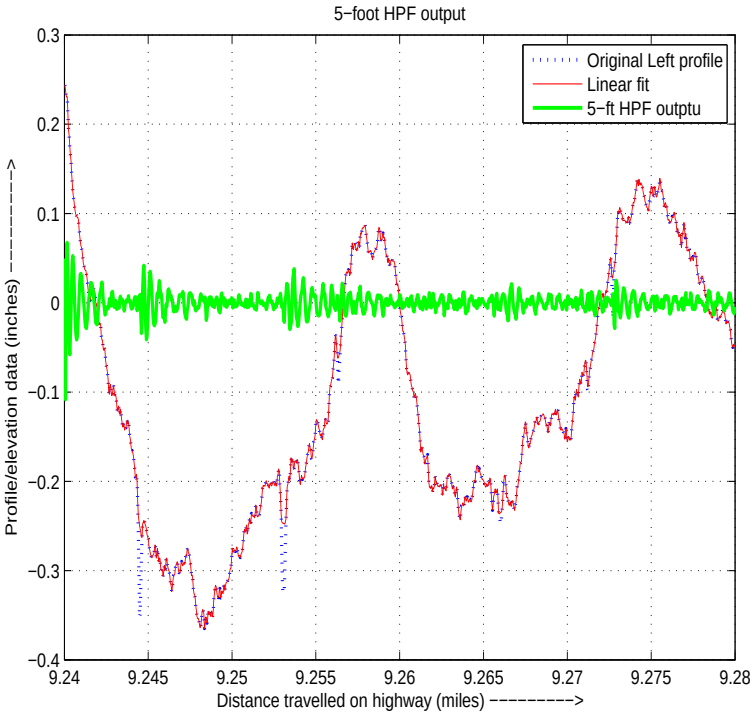

Figure 7.3: Filtered output using 5-foot Highpass filter

feature could nullify the uncertainty caused by the cutoff point of the filter.

The features that are currently being considered include the mean of the filtered output, the distance of the output values from the mean computed and the 'k' highest deviations on the filtered output. The value of 'k' is set based on a threshold which is a certain percentage of the maximum of the array of distances. For example, the result obtained with a threshold of 10 percent of the maximum is presented in figure 7.8.

From figure 7.8, it s observed that the peaks that appear significant in the third curve coincide precisely with those determined by the linear fit algorithm. In fact, the number of significant mile locations from the filter output is greater than that obtained from the linear fit. Some of the mile locations from the filter output are clustered around one peak/dip in the linear fit, which may be an indication of the

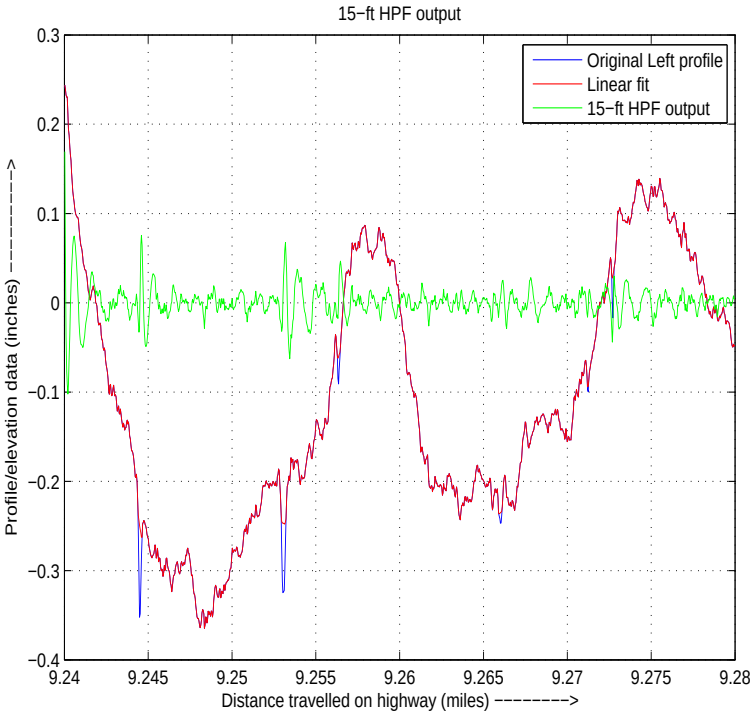

Figure 7.4: Filtered output using 15-foot Highpass filter

spread in the cracking phenomena over an area of the pavement surface rather than a discrete row. Hence, the distance of the filtered components from their mean may be a robust feature to determine the spread and hence, the severity of cracking.

7.2.3 Wavelet Analysis

Thirdly, the technique of time-frequency representation or wavelet decomposition is considered to process profile data. Wavelet transformation is a technique to identify the frequency characteristics of a signal, different from the traditional Fourier transform. The difference lies in the ability of the wavelet transform to represent the frequency components of a signal in both the time and frequency axes. Basically, in wavelet transformation, a mother wavelet is scaled and translated to yield short wavelet patterns that are used to represent the original signal. Applying multi-

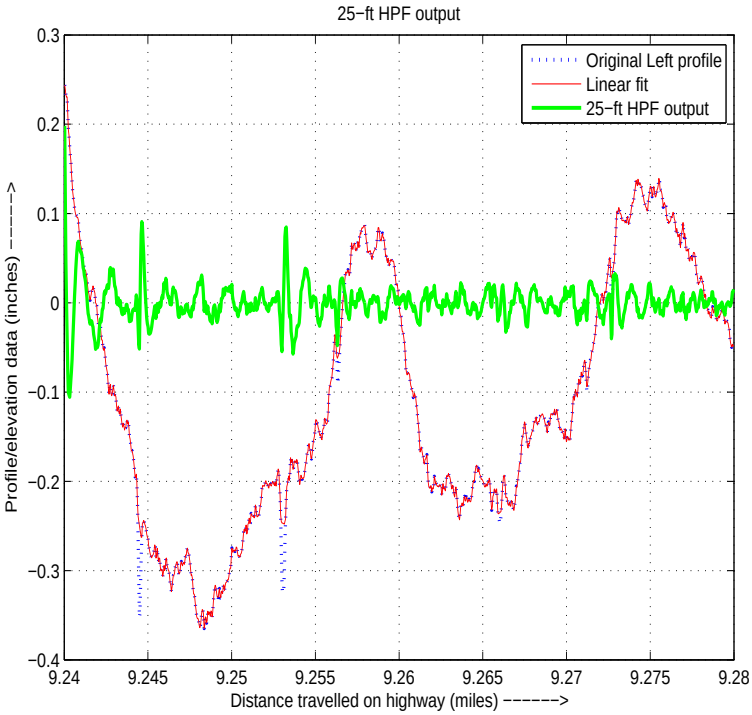

Figure 7.5: Filtered output using 25-foot Highpass filter

resolution analysis, the signal is resolved into multiple frequency subbands. Each subband identifies the signal components that correspond to the particular subband. The decomposition of the first level of wavelet coefficients further yield the coefficients at the second level and so on. For certain applications, multiple levels of decomposition may be required to precisely characterize the signal. The signal can be reconstructed by combining the weighted components from each level of resolution. Further discussion on wavelets can be found in [38].

In [36], the authors present the application of wavelet transformation to the analysis of pavement profiles to detect roughness. The method proposed is to decompose the signal into different levels of frequency components and scaling and combining them to reconstruct the original profile signal. The amount of scaling required on each frequency level indicates the contribution of that level to the reconstructed

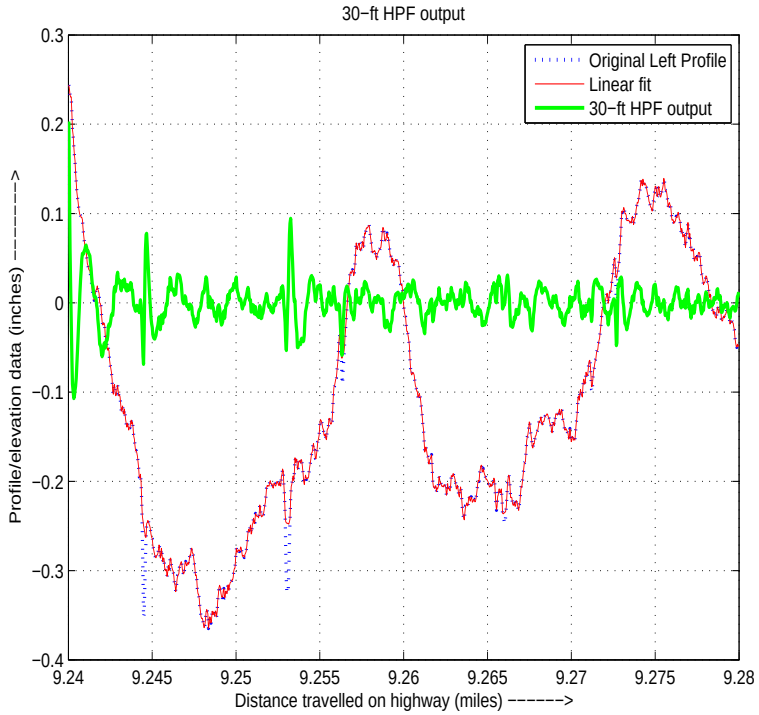

Figure 7.6: Filtered output using 30-foot Highpass filter

signal. Hence, the desired frequency components are obtained by thresholding the components in each level.

Techniques such as thresholding and filtering followed by wavelet decomposition are being considered to extract relevant information about cracking and its severity on the pavement images. In order to verify the output from wavelet analysis, it is compared with that obtained from linear fit and also with the actual cracks present in the corresponding pavement images. Figure 7.9 presents the first level of wavelet decomposition coefficients. The original profile and its linear fit are also presented as subplot 1 in 7.9. There are sudden peaks in the wavelet coefficient that coincide with deviations in the linear fit. But quantifying the peaks from a base level leads to uncertainties since the peaks are quite close to the average base level as per visual observation. Furthermore, the wavelet coefficients corresponding even to the

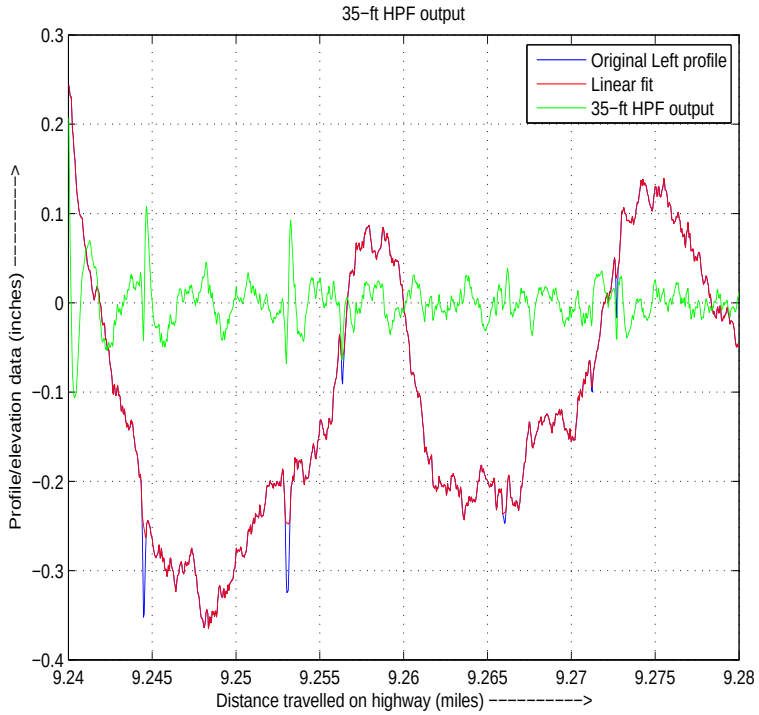

Figure 7.7: Filtered output using 35-foot Highpass filter

low frequency trends in the profile show certain peaks and dips. Hence, the reliability of wavelets in capturing cracking information is questionable. Further work in this regard will comprise of testing different types of wavelet functions and different levels of decomposition.

7.2.4 Recursive Least Squares(RLS) algorithm

The RLS algorithm is a linear prediction filtering technique which is commonly applied in the area of signal processing. The principle behind this algorithm is that the N^{th} sample of a data sequence is predicted from the previous $N-1$ samples by weighting them appropriately. The weights are developed iteratively by minimizing the residual error between the predicted and the actual values. In [39], the algorithm to implement this prediction filter and the parameters that affect convergence are

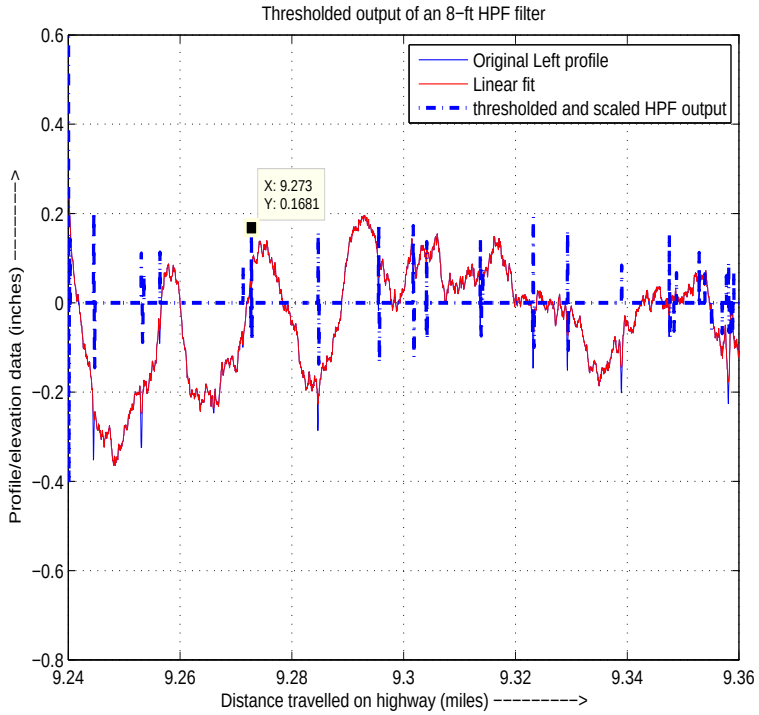

Figure 7.8: Thresholded output of an 8-foot Highpass filter

presented. Convolution of the weights developed with the original data signal yields the prediction error which captures any noisy spikes that affect the smooth trend of the signal. Since cracking phenomena on pavements correspond to deviations on the profile data depending on their code, the deviations can be considered as noisy spikes. Hence, the application of a prediction algorithm such as RLS could be expected to highlight the deviations from the low frequency trend in the profiles.

The results obtained upon application of RLS to a set of pavement profiles are presented in figure 7.10.

A 2−step algorithm is applied to the profile data, i.e., the algorithm is applied twice on the complete data set. The difference occurs in the initialization of the the constant λ and the inverse correlation matrix P. Initially, the value of λ is set between 0 and 1, closer to 1 and P is set to δ times the identity matrix, where

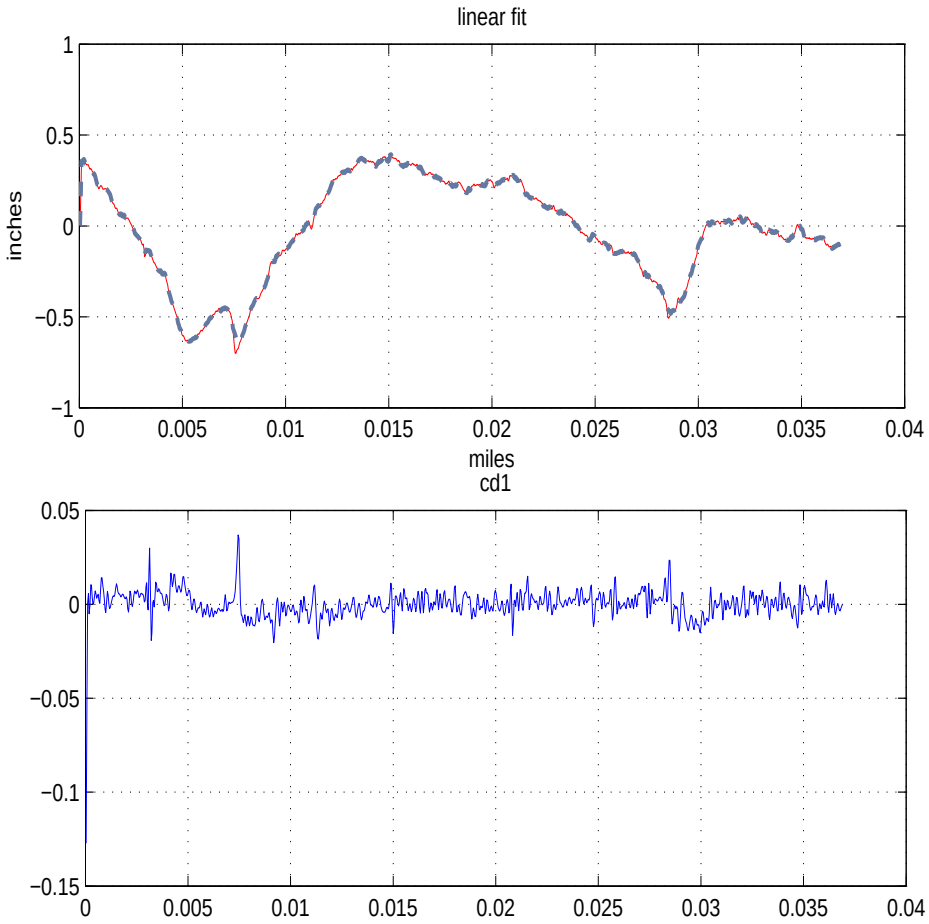

Figure 7.9: An example of application of wavelets to profiles

δ is a small positive value. When the algorithm is applied the first time, the values of λ and P are updated in each iteration. When the algorithm is applied to the complete data set for the second time, the recent updated values of λ and P are used as the initial values. As a result, the performance of the algorithm improves and the error signal is less noisier than at the end of the first application. In figure 7.10, λ is initialized with a value of 0.99 while P is initialized with 0.5 times the identity matrix. RLS develops an $L2$ type of solution, i.e., squared error minimization. Hence, the dominant characteristics that are emphasized are the high frequency spikes.

It is observed that, the high frequency deviations in the profile caused by

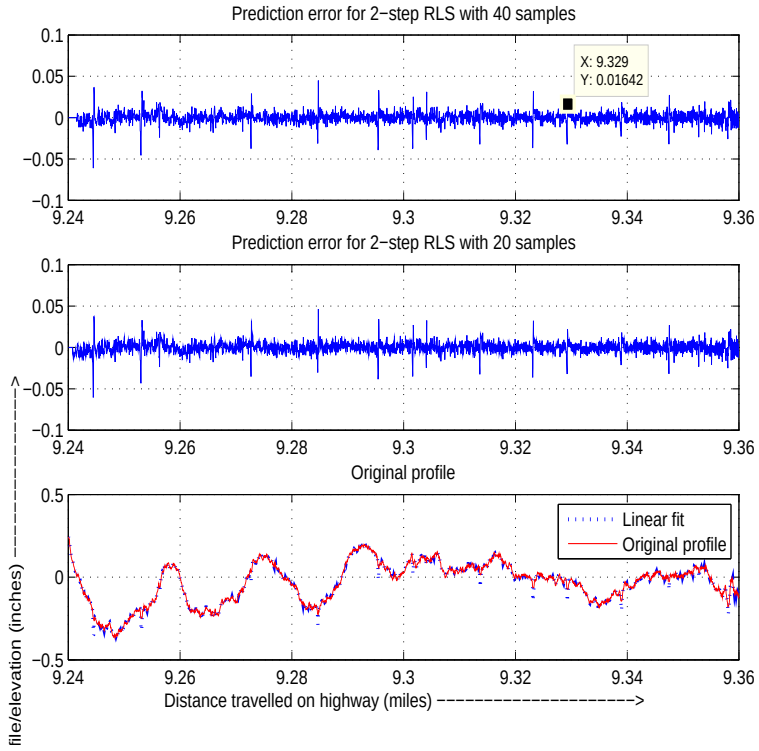

Figure 7.10: Prediction error from application of RLS algorithm to profile data

cracking manifest as sharp spikes in the prediction error. Upon comparison with linear fit, it appears that at all the points where linear fit indicates a crack, there are distinct dips and/or peaks in the error curve.

7.2.5 Iteratively Re-weighted Least Squares(IRLS) algorithm

IRLS is another linear prediction filter which provides an $L1$ type of solution, i.e. the absolute error is minimized and not its squared value. Similar to the RLS algorithm, appropriate weighting on the previous $N-1$ samples are determined to generate a prediction of the N^{th} sample. The IRLS algorithm not only generates the high frequency spikes, but it also emphasizes some of the low-frequency trends, thereby generating an error signal that appears slightly smoother than that generated by the RLS algorithm. The result of applying a 10−step IRLS algorithm on the profile in

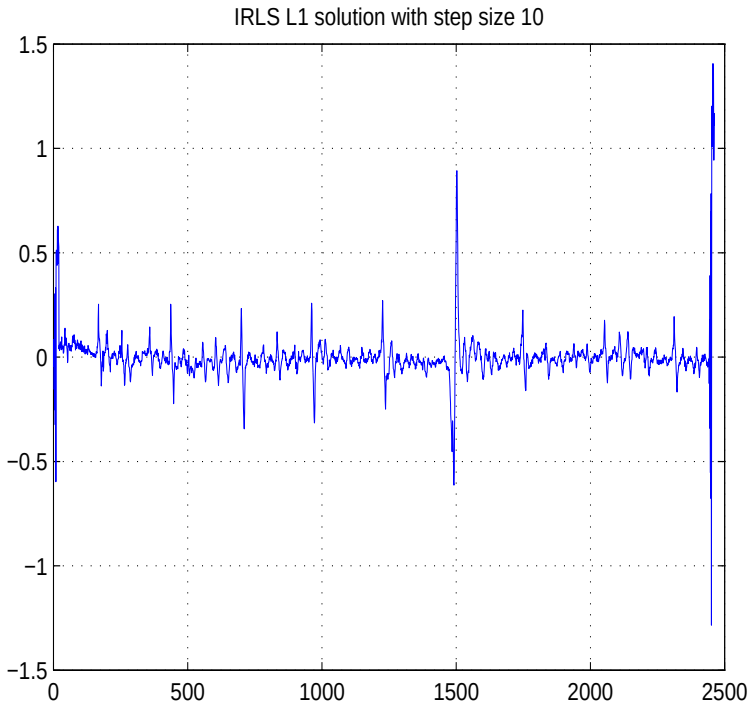

Figure 7.11: Prediction error from application IRLS algorithm to profile data

figure 7.12 is presented in figure 7.11. It is observed that the spikes that are visually observed in the original profile data appear as clear error signals in the convolved error output.

IRLS might be a more suitable algorithm to apply to profile data compared to the RLS algorithm due to its lower complexity. Furthermore, it is observed that the $L1$ type of solution might indicate the relatively sharp peaks more clearly with respect to the general trend in the data since it also retains some of this trend data in the final solution. However, deciding on appropriate thresholds to record only the relevant peaks in the error signal is a challenge yet to be resolved. The same issue is faced while considering the RLS algorithm as well. With proper thresholds, the error signal could be filtered such that sharp peaks are adequately extracted.

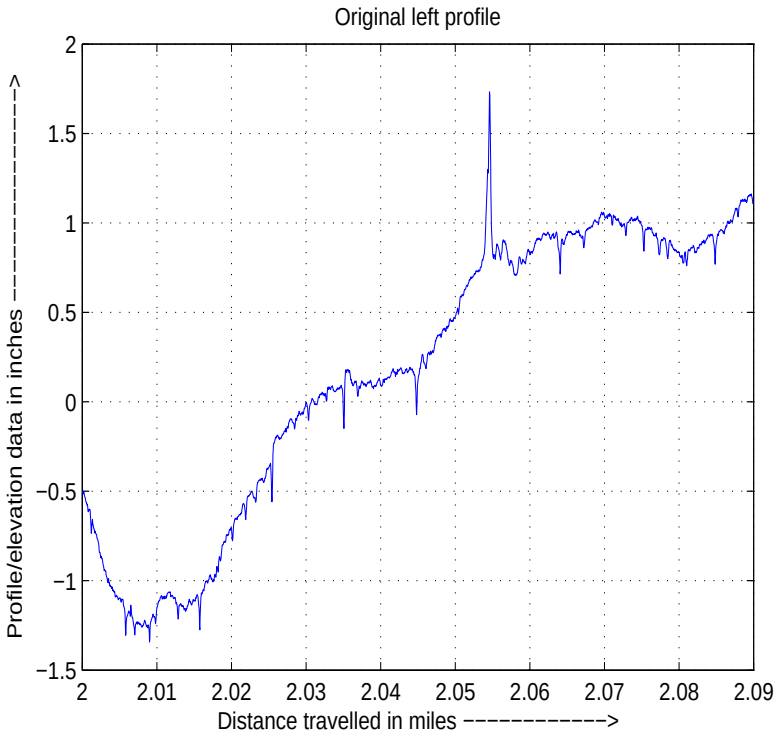

Figure 7.12: Original profile data

7.3 Unresolved Issues

The objective of analyzing pavement profile data is to extract information about cracking severity which could be used to classify cracks into codes. In order to associate the proper codes to the locations of cracks within the specific images, the row information obtained from image analysis is converted to a station number. This data is matched with appropriate profile values and hence the code and stored in a database for future retrieval. The challenges faced while implementing this association and are listed below.

- The profile data provided by KDOT contain an offset due to startup lags. Hence, the deviations caused by cracking are not precisely located and are observed to occur within some distance (around one-thousandth of a mile) of the original

crack locations.

- Some images do not have associated profile data, which could be attributed to halting the accelerometer while the camera continues to run.
- The base level relative to which the deviations can be identified is not definite for sets of images from different highway sections. Hence, non-adaptive base levels/thresholds could produce completely erroneous results for certain types of pavements. Appropriate base level and threshold setting would require observation and analysis of several sets of profile data.
- There is a lack of $TR - 2$ and 3 samples available and hence thresholds set to classify them are not accurate.

Currently, the research is oriented towards clarifying some of these issues, especially determining suitable thresholds and correct base levels. Future work regarding profile data and other aspects of the research are presented in the next chapter.

7.4 Summary

In this chapter, the analysis and characterization of pavement profile data was presented. Significant information about pavement roughness, crack severity and locations can be extracted from the profile data. Hence, analyzing profile data and integrating crack severity information to the results of image analysis are important research objectives. The current focus of the research is on techniques that may be appropriate for processing profile data. Future research objectives and conclusions of the thesis are presented in the next chapter.

Chapter 8

Conclusion

In the previous chapter, we presented a brief discussion on integrating the profile data and the unresolved issues associated with it. In this chapter, the key contributions of this work are summarized. Finally, future work to extend the project is identified.

8.1 Summary of key contributions

In this thesis, an *automated* pavement distress detection and classification algorithm is developed. The technique of Principal Component Analysis is applied to pavement images to extract characteristic features of cracks at the subimage level. Classification at three levels is considered : 1) Pixel level, 2) Subimage level and 3) Image level. Noisy pavement images are repeatedly filtered at different stages such that the false detection rate is highly controlled. In the detection/preprocessing stage, thresholding is used to remove most of the non-cracked pixels so that further processing is accurate. The recognition stage classifies subimages as cracked/non-cracked and the structure of the cracking in an image is developed. Finally, postprocessing is performed on the image to establish connectivity among subimages and present a well-segmented image to the end analyst. The complete algorithm is automated and hence, minimal/no

human interaction is required to process 1000s of pavement images. In addition, transverse cracks are detected with a high rate of detection. The algorithm can also detect longitudinal cracking and hence can be extended to detect block cracking as well.

The classification of cracks as sealed/unsealed is implemented using the technique of cumulative Fourier transform of a subimage. Sealed/unsealed classification indicates the condition/status of a crack. Hence, the importance of this level of classification lies in the requirement to determine repair needs for different cracks. Furthermore, integration of information about the sealed/unsealed nature of a crack with the pavement profile data yields the code of the crack. Thus, the Fourier based classification of cracks is one of the key contributions of this thesis. Finally, the initiative on the analysis of profile data to determine the severity of cracking, in order to classify transverse cracks based on codes is a significant discussion in this thesis. Some of the techniques under consideration to process profile data are presented and the direction of future work in this regard is indicated.

Several image examples are provided to exemplify the performance of the developed algorithm. The image results and detection and false alarm probabilities are found to be highly encouraging. A mathematical construct is provided where pertinent, especially with regard to the development of the subimage classification stage. The profile-based results obtained so far appear promising as well, in the sense that, a high percentage of the cracking information is captured by significant deviations in the processed results. Hence, with some fine-tuning, meaningful information that can be accurately associated with image-based results can be extracted from the pavement profiles.

8.2 Future Work

The future focus of the research is presented below.

- This thesis presents the automated detection of transverse and longitudinal cracking, with emphasis on the former type of cracks. Though block cracks are combinations of the first two types, specific inter-connection/loop algorithms may be required for accurate detection of block cracks. The algorithm may also be extended to detect Fatigue/alligator cracks. These are the more severe cracking phenomena which have to be detected in a timely manner.

- The conversion of the platform used to implement the algorithm from Matlab to C would improve the computational time greatly. Hence, this conversion is a potential expansion to the thesis.

- Perfecting the technique for analysis of pavement profile data such that it is effective on various sections of the highway would be an important development in the research. Integrating this technique with the information from the image processing algorithm would present self-validating results to the end analyst, reducing much of the labor otherwise involved in manually analyzing images and profiles simultaneously.

- Invoking a software such as Google Earth at the end of the algorithm can present geographical locations along the Kansas highways where cracking is present. Furthermore, using Automatic Report Generation (ARG), the location, classification, severity and geometric characteristics of every crack along Kansas highways can be automatically generated and stored. This can in turn reduce the cost and time involved in monitoring the status of highways.

References

[1] "Distress identification manual for the long-term pavement performance program (fourth revised edition)," *FHWA-RD-03-031*.

[2] C. Scheffy and E. Diaz, "Asphalt concrete fatigue crack monitoring and analysis using digital image analysis techniques," in *Accelerated Pavement Testing* 1999 *International Conference*, October 1999.

[3] T. Yamaguchi, S. Nakamura, R. Saegusa, and S. Hashimoto, "Image-based crack detection for real concrete surfaces," in *IEEJ Transactions On Electrical And Electronic Engineering*, vol. 3, 2008, pp. 128–135.

[4] Y. Fujita, Y. Mitani, and Y. Hamamoto, "A method for crack detection on a concrete structure," in *The 18th International Conference on Pattern Recognition*, 2006.

[5] T. C. Hutchinson and Z. Chen, "Improved image analysis for evaluating concrete damage," in *Journal Of Computing In Civil Engineering*, May/June 2006.

[6] E. Teomete, V. R. Amin, H. Ceylan, and O. Smadi, "Digital image processing for pavement distress analyses," in *Proc. of the 2005 Mid-Continent Transportation Research Symposium*, Ames,Iowa, Aug 2005.

[7] B.Xu and Y.Huang, "Automatic inspection of pavement cracking distress," in *Proc. of SPIE*, vol. 5909, 2005.

[8] J. Bray, B. Verma, X. Li, and W. He, "A neural network based technique for automatic classification of road cracks," in *IEEE International Joint Conference on Neural Networks*, July 2006.

[9] "http://www.roadware.com/software/wisecraxnt/."

[10] H.D.Cheng and C. Glazier, "Automated real-time pavement crack detection and classification system," in *Final Report for Highway IDEA Project 106, Transportation Research Board, Washington, D.C.*, January 2007.

[11] H.D.Cheng and M.Miyojim, "Novel system for automatic pavement distress detection," in *Journal of Computing in Civil Engineering*, vol. 12, July 1998.

[12] W. Xiao, X. Yan, and X. Zhang, "Pavement distress image automatic classification based on density-based neural network," in *Lecture Notes in Computer Science, Pattern Recognition*, September 2006, pp. 685–692.

[13] J. Chou, W.A.O'Neill, and H.D.Cheng, "Pavement distress classification using neural networks," in *Systems, Man, and Cybernetics, 1994. 'Humans, Information and Technology'., 1994 IEEE International Conference*, vol. 1, San Antonio, TX, Oct 1994, pp. 397 – 401.

[14] S. Iyer and S. K. Sinha, "Segmentation of pipe images for crack detection in buried sewers," in *Computer-Aided Civil and Infrastructure Engineering*, 2006.

[15] "Introduction to crack sealing," in *Road Management and Engineering Journal, Sheet* 69, Spring 1997.

[16] "Highway performance monitoring system. field manual for the continuing analytical and statistical data base," in *Federal Highway Administration*, 1984.

[17] K. D. of Transportation, "Section iv - pavement surface condition rating procedure," in *Manual for Pavement Distress Survey and Rating.*

[18] J. B. P.E., "A synopsis on the current equipment used for measuring pavement smoothness," *Federal Highway Administration, Pavements*, August 2001.

[19] K. Rajan, D. D.Day, and B. Natarajan, "Detection and classification of pavement distress via principal component analysis and sensor fusion techniques," *submitted to the journal El Sevier(DSP)*, 2008.

[20] "Imaging vehicle operation manual (draft)," in *International Cybernetics Corporation, Largo, Florida*, January 2004.

[21] "http://en.wikipedia.org/wiki/pixel."

[22] "http://www.cs.dartmouth.edu/farid/tutorials/fip.pdf."

[23] R. C. Gonzalez and P. Wintz, *Digital Image Processing.* Addison-Wesley Pub. Co., Advanced Book Program, 1977.

[24] A. Ito, Y. Aoki, and S. Kashimoto, "Accurate extraction and measurement of fine cracks from concrete block surface image," in *Proc. of IEEE*, 2002.

[25] H. N. Koutsopoulos, I. E. Sanhouri, and A. B. Downey, "Analysis of segmentation algorithms for pavement distress images," in *Journal of Transportation Engineering*, vol. 119, no. 6, November/December 1993.

[26] D. H. Kil and F. B. Shin, "Automatic road-distress classification and identification using a combination of hierarchical classifiers and expert systems-subimage and object processing," in *Iternational Conference on Image Processing,* IEEE Proc., vol. 2, October 1997, pp. 26–29.

[27] "csnet.otago.ac.nz/cosc453."

[28] S. Hermosilla-Lara, P. Joubert, D. Placko, F. Lepoutre, and M. Piriou, "Enhancement of open-cracks detection using a principal component analy-

sis/wavelet technique in photothermal non-destructive testing," in *Proceedings of the International QIRT Conference, Dubrovnik*, September 2002, pp. 41–46.

[29] J. Peyton Z. Peebles, "Probability, random variables and random signal principles, fourth edition," in *McGraw-Hill, Inc.*, 2001.

[30] H. V. Poor, "An introduction to signal detection and estimation, second edition," in *Springer-Verlag*, 1994.

[31] "http://en.wikipedia.org/wiki/sensorfusion."

[32] "www.ph.tn.tudelft.nl/courses/fip/noframes/fip-morpholo.html."

[33] T. Esselman and J. Verly, "Some applications of mathematical morphology to range imagery," in *Acoustics, Speech, and Signal Processing, IEEE International Conference on ICASSP*, vol. 12, April 1987, pp. 245–248.

[34] D. Grivas, C. Bhagvati, M. Skolnick, and B. Schultz, "Feasibility of automating pavement distress assessment using mathematical morphology," in *Transportation Research Record*, 1994, pp. 52–58.

[35] D. D.Day and D. Rogers, "Fourier-based texture measures with application to the analysis of the cell structure of baked products," in *Digital Signal Processing*, vol. 6, no. 3, July 1996, pp. 138–144.

[36] J. Pont and A.Scott, "Beyond road roughness-interpreting road profile data," in *Road and Transportation Research*, March 1999.

[37] J. J. Zhu and W. Zhu, "Stochastic modeling of pavement roughness," in *IEEE Proceedings of the Twenty-Eighth Southeastern Symposium on System Theory*, April 1996, pp. 28–32.

[38] R. Polikar, "The wavelet tutorial," in *Fundamental Concepts and an Overview Of The Wavelet Theory*, November/December 1994.

[39] S. Haykin, "Adaptive filter theory, third edition," in *Prentice Hall, New-Jersey*, 1996.